Analysis of family reflections of OD mica polytypes, and its application to twin identification

Massimo Nespolo

MINERALOGICAL JOURNAL, VOL. 21, No. 2, pp. 53 – 85, APRIL 1999

Analysis of family reflections of OD mica polytypes, and its application to twin identification

Massimo NESPOLO

Mineralogical Institute, Graduate School of Science, University of Tokyo, 7-3-1 Hongo, Bunkyo-ku, Tokyo 113-0033, Japan.
Present address: National Institute for Research in Inorganic Materials, Research Center for Creating New Materials, 1-1 Namiki, Tsukuba-shi, Ibaraki 305-0044, Japan.

Abstract:

The Periodic Intensity Distribution (PID) analysis of the diffraction pattern of mica polytypes can be applied to single crystals. Since micas often appear as twins, general criteria are established to investigate the presence of twinning. These criteria are derived through a geometrical approach based on the general symmetry features of the layer stacking. Non-orthogonal polytypes have been classified into *Class a* and *Class b*, depending on the direction along which *c* axis is inclined. Common twinning in micas is by reticular pseudo-merohedry; for *Class a* polytypes its presence can be recognized by careful inspection of the geometry of the diffraction pattern. On the other hand, a pseudo-rhombohedral primitive cell exists in case of *Class b* polytypes: for them, two of the five pairs of twin elements common to non-orthogonal polytypes correspond to twinning by pseudo-merohedry, which does not modify the geometry of the diffraction pattern.

It is proved that the geometrical features of mica diffraction pattern can be divided into two types: 1) the number and position of diffractions common to all polytypes built on the same structural principle, called *family reflections*, derived by calculating the reflection conditions; 2) the number of planes with orthogonal geometry. The analysis takes into account that most of the mica polytypes reported to date are *OD structures* belonging to two *subfamilies*, and that a third, rare kind of polytypes, called *mixed-rotation polytypes*, consists instead of *non-OD structures*. For mixed-rotation polytypes the definition of the family reflections differs from that of the two subfamilies. It is shown that these three kinds of polytypes are easily recognized by analyzing the reflections with $h \neq 0 (\mathrm{mod}\ 3)$ and $k = 0 (\mathrm{mod}\ 3)$. Then, the number of reflections along family rows and the number of orthogonal planes in the diffraction pattern permit to investigate the presence of twinning.

1. Introduction

Mica polytypes represent one of the most complex groups of structures in nature. Because of the large number of stacking possibilities, which increases very rapidly with the number of layers in the repeat unit (Mogami *et al.*, 1978; McLarnan, 1981), and of the existence of pseudo-symmetries (Bailey, 1975), both the geometrical description and the interpretation of the diffrac-

tion patterns is rather difficult. Partial enhancement of symmetry has been observed too (Sadanaga and Takeda, 1968). This situation is made even more complex by the occurrence of twins. The diffraction pattern of twins is often hardly distinguishable from that of polytypes (Sadanaga and Takéuchi, 1961; Nespolo *et al.*, 1997a,b; Nespolo and Kogure, 1998), and for this reason Takano and Takano (1958) introduced the definition of *apparent polytypism*. Several approaches have been developed to reach a general, systematic and as simple as possible interpretation, and different authors have recognized different and not always equivalent basic features, common to all or part of the polytypes. Some features of the lattice and/or of the intensity distribution can be explained in a different way by those approaches; depending upon the purpose, one method may be more suitable than the others. In this paper, a detailed analysis of the symmetry principles and of the geometry of the diffraction pattern of mica polytypes is presented; the reflection conditions for the so-called *family reflections*, which are common to all polytypes built on the same structural principle, are analytically derived. The results lead to: 1) classify polytypes into three kinds, easily recognized from the geometry of the diffraction pattern; 2) reveal the existence of a pseudo-rhombohedral primitive cell for one of the two *Classes* in which non-orthogonal polytypes are subdivided; 3) re-investigate the twin laws of non-orthogonal mica polytypes; 4) introduce general criteria that permit to confirm or exclude the presence of twinning by reticular pseudo-merohedry through a simple inspection of the geometry of the diffraction pattern. The procedure to solve the stacking sequence of an unknown mica polytype is outlined.

2. Choice of the Unit Layers

Micas are phyllosilicates built by stacking two tetrahedral sheets (*T*) sandwiching an octahedral sheet (*O*). Monovalent and, less frequently, divalent cations take place between two adjacent *T* sheets belonging to next layers (Pauling, 1930). Since the cleavage plane in micas is commonly thought to be in correspondence of the cations between two next *T* sheets (Müller and Chang, 1969; Kogure, 1997), the sequence *T-O-T* is the most commonly adopted unit layer (conventional layer). Following Takéuchi (1971) and Takéuchi and Haga (1971), hereafter it is labelled *M layer*. The two *T* sheets within a layer are staggered by |*a*|/3, in the (001) projection and the highest symmetry of the whole *M* layer is *C2/m* (Pabst, 1955). However, both the *T* and the *O* sheets have symmetry higher than the *M* layer.

In the octahedral sheet three cation sites exist: one site is trans-coordinated by OH/F and is labelled *M*1; the other two sites are cis-coordinated by OH/F and are labelled *M*2. Depending whether two or all of the three sites are occupied, micas are divided into *dioctahedral* and *troctahedral* (Smith and Yoder, 1956). Then, the symmetry of the *O* sheet can be $H(\bar{3})1m$ (*homo-octahedral micas*: all the three sites occupied by the same cation), $P(\bar{3})1m$ (*meso-octahedral micas*: two of the three sites occupied by the same cation; the remaining one may be vacant) or *P*(3)12 (*hetero-octahedral micas*: the three sites are occupied in a different way) (Ďurovič, 1994a) [layer-group notation after Dornberger-Schiff (1959); details in Merlino (1990)]. In hetero-octahedral micas the cis-sites are subdivided into two sites *M*2 and *M*3 (Bailey, 1984). For meso-octahedral micas, the origin of the *O* sheet is in the site with different occu-

pation; for hetero-octahedral micas it is in the site containing the lowest electron density (Ďurovič *et al.*,1984). The direction connecting two *M*1 sites defines the *a* axis; normal to it the *b* axis is located, and the orthohexagonal relation $b = a3^{1/2}$ is closely followed.

Two models have been proposed to describe the symmetry and the main structural features of the *T* sheets. In the *Pauling model* all the geometrical distortions are neglected and the *T* sheets have ideal layer-symmetry *P*(6)*mm* (Pauling, 1930). The most relevant distortion of the *T* sheets is the ditrigonalization effect, which reduces the tetrahedral layer-symmetry to *P*(3)1*m*. This arrangement is described by the *trigonal model* [*1] (Nespolo *et al.*, 1999b). In Pauling model, the coordination polyhedron for interlayer cations is a hexagonal prism, which is not modified by a *n*60° rotation between next layers. On the other hand, in the trigonal model rotations by 2*n*60° lead to a trigonal antiprismatic coordination for interlayer cations, whereas rotations by (2*n*+1)60° to trigonal prismatic coordination (Zvyagin, 1957; Radoslovich, 1959). In Fig. 1 a comparative view of different unit layers is given.

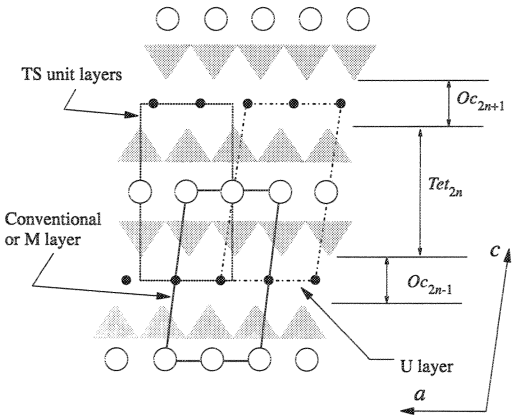

FIG. 1. (010) projection showing the schematic structure of micas and the choice of some alternative unit layers. *U*-layer is defined in Takéuchi (1971) and in Takéuchi and Haga (1971), TS unit layers in Sadanaga and Takeda (1969) and in Takeda and Sadanaga (1969), *Oc* and *Tet* are OD layers (Dornberger-Schiff *et al.*, 1982). White circles: interlayer cations. Small black circles: octahedral cations. Gray triangles: coordination polyhedra around tetrahedral cations. The view along *c* is compressed because of drawing necessities.

3. Reticular Classification of Mica Polytypes: Unit Cells, Axial Settings and Pseudo-Symmetries

Hereafter, a pair of pseudo-orthohexagonal axes (*a, b*) and a pair of pseudo-hexagonal axes (a_1, a_2) in the (001) plane of mica layer are used. Among the three independent relative orientations of these two pairs, the one in which *a* and a_1 axes coincide is here taken (see Fig. 2 in Nespolo *et al*, 1997a). The corresponding orthohexagonal cell is labelled C_1 in Arnold (1996)[*2] and on it a (pseudo)-orthohexagonal axial setting is built, which has been labelled C_1 too (Nespolo *et al.*, 1997a, 1998). The (001) projection of *c* axis is labelled $\mathbf{c}_n$

[*1] The trigonal model is also known as *Radoslovich model* (Radoslovich, 1961), but it was proposed for the first time by Belov (1949).

[*2] Three orthohexagonal cells are described in Arnold (1996), namely C_1, C_2, and C_3. The orthohexagonal cell used since long ago in describing micas corresponds to C_1 (*e.g.* Donnay *et al.*, 1964). Other authors, such as the OD school, adopted the C_2 cell (*e.g.* Ďurovič *et al.*, 1984). This different choice of the orthohexagonal cell has to be taken into account when comparing the descriptions given by different authors.

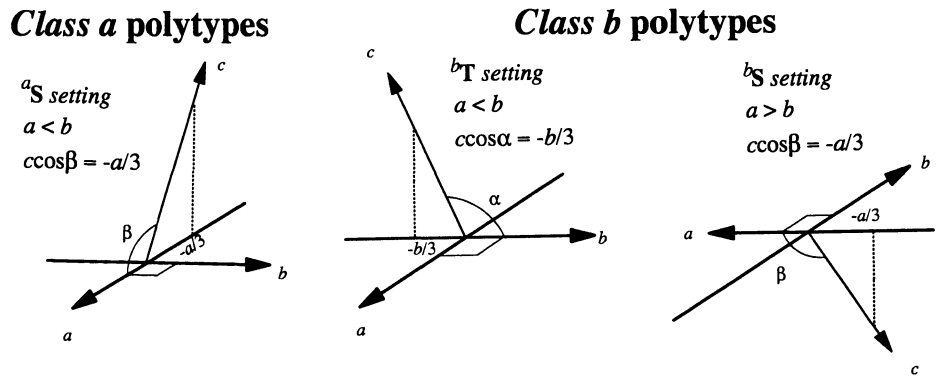

FIG. 2. Definition of the ^{a}**S**, ^{b}**T** and ^{b}**S** axial settings of mica polytypes.

(Zvyagin, 1997). With reference to (*a, b*) axes, mica polytypes have been classified as follows:

1. orthogonal mica polytypes have $\mathbf{c}_n$= (0, 0) and can be hexagonal (no known examples), trigonal and orthorhombic;
2. non-orthogonal polytypes are divided into *Class* a [$\mathbf{c}_n = (x_n, 0)$] and *Class b* [$\mathbf{c}_n = (0, y_n)$]; the lattice of triclinic polytypes is metrically (pseudo)-monoclinic.

The number of layers building a polytype is expressed as:

$$N = 3^n(3K+L) \qquad (1)$$

(*K* and *n* are non-negative integers; *L*=1 or 2). *n* defines the *Series* and *L* the *Subclass*. *K* is a constant that enters in the transformation matrices relating axial settings (Nespolo *et al.*, 1997a, 1998).

For non-orthogonal polytypes, the (ideal) length of $\mathbf{c}_n$ is either *a*/3 or *b*/3 (Zvyagin, 1967); it follows that the period along *c* in the C_1 setting (orthogonal setting) corresponds to 3*N* layers. The following symbols are used hereafter:

c^*_1 : parameter along c^* of the simplest polytype (1*M*): it corresponds to about 0.1Å^{-1};

N: number of layers in the conventional cell;

N': number of layers in the unit cell of the C_1 setting: *N'* = *N* for orthogonal polytypes, *N'* = 3*N* for non-orthogonal polytypes;

l_{C_1}: *l* index in the C_1 setting.

Several monoclinic settings, whose cell contains a single repeat unit (*N* layers), can be chosen for non-orthogonal polytypes. Among them, the setting in which $\mathbf{c}_n$ is kept (ideally) constant for all polytypes is labelled ^{a}**S** [*Class a*: $\mathbf{c}_n = (\bar{1}/3, 0)$; **S** stands for *Standard*] and ^{b}**T** [*Class b*: $\mathbf{c}_n = (0, \bar{1}/3)$; **T** stands for *Transitional*]. The corresponding monoclinic *l* indices are labelled $l_{a\mathbf{S}}$ and $l_{b\mathbf{T}}$ (Nespolo *et al.*, 1997a). The metric equations in both direct and reciprocal space and the relations between *l* and *h, k* indices are given in Table 1. The ^{b}**T** setting is monoclinic *a*-unique; from it, a monoclinic *b*-unique setting is obtained through the axes exchange $a \rightarrow -b$; $b \rightarrow -a$; $c \rightarrow -c$, so that $a > b$ and $\beta > 90°$, as in Smith and Yoder (1956) definition: this setting is labelled ^{b}**S** (Fig. 2).

TABLE 1. Metric equation in direct and reciprocal space and relation between Miller indices in the orthogonal and monoclinic settings for the two *Classes*.

Class	Metric equations in direct space	Metric equations in reciprocal space	relation between l_{C_1} h, and k indices	relation between orthogonal and monoclinic l indices
a	$c\cos\beta = -a/3$	$a^*\cos\beta^* = c^*/3$	$l_{C_1} = h(\text{mod } 3)$	$l_{a_S} = (l_{C_1} - h)/3$
b	$c\cos\alpha = -b/3$	$b^*\cos\alpha^* = c^*/3$	$l_{C_1} = k(\text{mod } 3)$	$l_{b_T} = (l_{C_1} - k)/3$

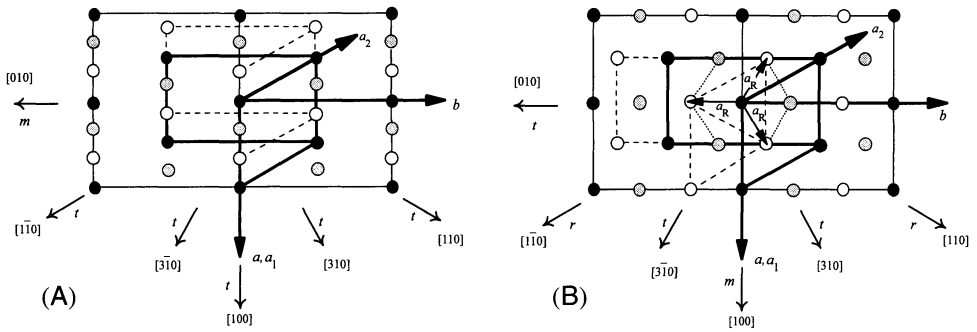

FIG. 3. Projection on (001) plane of the primitive, conventional (double), pseudo-hexagonal (triple) and C_1 (sextuple, pseudo-orthohexagonal) cells, for *Class a* (A) and *Class b* (B) polytypes. Black, white and gray circles represent lattice nodes at $z = 0$, 1/3 and 2/3 (z is referred to c axis of the C_1 cell). Thick lines: borders of the C_1 cell and of the pseudo-hexagonal cell. Dashed lines: borders of the upper plane of the conventional and primitive cells (the lower plane is in common with C_1 cell and pseudo-hexagonal cell respectively). For *Class b* a pseudo-rhombohedral cell exists (dotted lines), which is best viewed by means of the pseudo-rhombohedral axes a_R. a, b: (pseudo)-orthohexagonal axes. a_1, a_2: (pseudo)-hexagonal axes. The (pseudo)-two-fold axes in the (001) plane of the pseudo-hexagonal multiple lattice are indicated by an arrow, according to *International Tables for Crystallography* convention. For non-orthogonal polytypes they are classified in the following way. ***m***: structure two-fold axis for monoclinic polytypes belonging to crystal classes 2 and 2/*m*; merohedry twin axis for monoclinic polytypes belonging to crystal class *m* and for triclinic, metrically monoclinic polytypes; pseudo-merohedry twin axis for metrically triclinic polytypes. ***t***: reticular pseudo-merohedry twin axes for both monoclinic and triclinic polytypes. ***r***: pseudo-merohedry twin axes for both monoclinic and triclinic polytypes (only *Class b*). The same classification holds for the planes normal to (001) (not shown).

Three unit cells, built on the two pairs of axes described above, are useful to put in evidence the existence of pseudo-symmetries.

1. The (ideally) orthohexagonal cell of the C_1 setting. For non-orthogonal polytypes it is a sextuple cell; for orthogonal polytypes it is a double cell that coincides with the conventional cell. It is also the cell of the twin lattice, in case of twinning by reticular pseudo-merohedry (Donnay *et al.*, 1964).
2. A pseudo-hexagonal cell based on (a_1, a_2) axes. For non-orthogonal polytypes it is a triple cell; for orthogonal polytypes it is primitive.
3. The conventional cell (double cell), monoclinic *C* centred. For orthogonal polytypes it coincides with the C_1 cell. For non-orthogonal polytypes, by stacking three conventional

TABLE 2. Cell parameters of refined *Class b* mica polytypes. Cell parameters have been obtained from those of the conventional cell by linear transformation of the metric matrices. Transformation matrices are given in Nespolo *et al.*, (1998) (conventional to C_1 cell), and Arnold (1996) (C_1 to pseudo-hexagonal and pseudo-hexagonal to pseudo-rhombohedral). Cell parameters and cell volume for the reduced cell have been calculated according to LePage (1982).

Polytype	Cell[§]	a(Å)	b(Å)	c(Å)	α(°)	β(°)	γ(°)	V(Å^3)
	cc	5.200	9.032	20.15	99.77	90.00	90.00	932.6
	C_1	5.200	9.032	59.59	91.18	90.00	90.00	2798.1
$2M_2$[1]	pHc	5.200	5.211	59.59	91.02	90.00	119.93	1399.1
	pRc	20.057	20.057	20.15	14.89	14.89	14.90	466.3
	rc	5.200	5.211	20.06	83.57	82.55	60.07	466.3
	cc	5.175	8.965	20.31	100.67	90.00	90.00	926.0
	C_1	5.175	8.965	59.92	92.21	90.00	90.00	2777.9
$2M_2$[2]	pHc	5.175	5.176	59.92	91.92	90.00	120.00	1388.9
	pRc	20.139	20.139	20.31	14.70	14.70	14.76	463.0
	rc	5.175	5.176	20.14	84.53	82.62	60.01	463.0
	cc	5.226	9.076	21.41	99.48	90.00	90.00	1001.6
$2M_2$[3]	C_1	5.226	9.076	63.37	91.36	90.00	90.00	3004.9
	pHc	5.226	5.237	63.37	91.18	90.00	119.93	1502.6
	pRc	21.303	21.303	21.41	14.08	14.08	14.09	500.8
	rc	5.226	5.236	21.30	84.12	82.95	60.07	500.8
	cc	5.350	9.276	30.17	95.72	90.00	90.00	1489.8
	C_1	5.350	9.276	90.06	89.84	90.00	90.00	4469.4
$3A_1$[4#]	pHc	5.350	5.354	90.06	86.86	90.00	120.12	2226.9
	pRc	30.183	30.183	30.17	10.18	10.18	10.17	744.9
	rc	5.350	5.354	30.17	94.95	90.00	119.97	744.9
	cc	5.350	9.270	30.17	95.84	90.00	90.00	1488.5
	C_1	5.350	9.270	90.04	89.96	90.00	90.00	4465.5
$3A_1$[5]	pHc	5.350	5.352	90.04	89.97	90.00	119.99	2233.0
	pRc	30.17	30.17	30.17	10.18	10.18	10.17	744.3
	rc	5.350	5.352	30.17	95.06	90.00	119.99	744.2
	cc	5.328	9.228	59.71	92.95	90.00	90.00	2931.9
	C_1	5.328	9.228	178.89	90.00	90.00	90.00	8795.4
$6A_1$[6]	pHc	5.328	5.328	178.89	90.00	90.00	120.00	4379.8
	pRc	59.71	59.71	59.71	5.11	5.11	5.11	1467.5
	rc	5.328	5.328	59.71	87.45	87.45	60.00	1466.1

[§]cc: conventional cell; pHc: pseudohexagonal cell (hexagonal axes); rc: reduced cell (Le Page, 1982); pRc: pseudo-rhombohedral cell (rhombohedral axes). [1]Takeda and Burnham (1969); [2]Zhukhlistov *et al.* (1973); [3]Ni and Hughes (1996); [4]Ross *et al.* (1966); [5]Borutskiy *et al.* (1987); [6]Zhukhlistov *et al.* (1993) (Z symbols: 626264). [#]Angular parameters modified from Ross *et al.* (1966), as described in the text.

cells along c axis the C_1 cell is obtained.

Successive lattice planes are shifted by 1/3 of the short (*Class a*) and long (*Class b*) diagonal of the two-dimensional mesh built on (a_1, a_2) axes. Therefore, for *Class b* polytypes a pseudo-rhombohedral primitive cell can be chosen, having (almost) the same volume of the reduced cell (Fig. 3B). In Table 2 the cell parameters for the above-listed three cells, the pseudo-rhombohedral cell and the reduced cell are calculated for three examples of $2M_2$ polytype, two examples of $3A_1$ polytype and one example of $6A_1$ polytype, starting from the refined conventional cells, as taken from the literature. Notwithstanding the different crystal chemistry, the pseudo-rhombohedral symmetry is followed even more closely

than the other approximated symmetries. The general reflection conditions for the rhombohedral lattice in hexagonal axes are: $-h+k+l = 3n$. When expressed in the C_1 setting, they become: $-3h+k+2l = 6n$. Taking into account the C centring condition, they correspond to $l(\text{mod } 3) = k(\text{mod } 3)$ [$l = k(\text{mod } 3) + 3n$, n integer], which is just an alternative expression of the condition of integrality of monoclinic indices given in Table 1 for $^b\mathbf{T}$ setting.

4. Mica Polytypes as OD Structures: Superposition Structures, Family Structure and Family Reflections.

If the position of a layer is uniquely defined by the position of the adjacent layers and by the so-called *vicinity condition* (*VC*), which states the geometrical equivalence of layer pairs, the resulting structure is fully ordered. If, on the other hand, more than one position is possible that obeys the VC, the resulting structure is an *OD structure*[*3] and the layers building it are called *OD layers*. The choice of the OD layers in general is not absolute (Grell, 1984). Both fully ordered structures and OD structures share the common name of *VC structures* (Dornberger-Schiff, 1964, 1966, 1979; Ďurovič, 1997). While OD structures are polytypes, not all polytypes may be considered OD structures, since not all polytypes obey the *VC* (Zvyagin, 1993).

All OD structures, even of different substances, built according to the same symmetry principle, belong to an *OD groupoid family*: this is an abstract family, whose members are the groupoids describing the symmetry of the substances sharing the same symmetry principle. Then, the OD structures of the same substance built on the same structural principle belong to one and the same *family:* the members of a family are individual, real structures (Ďurovič and Weiss, 1986). *Superposition structure* is called a fictitious, average structure obtained from a Fourier series calculated with a three-dimensional subset of diffractions corresponding to a subgroup of translations in the reciprocal lattice. An *n-fold* superposition structure is obtained from a translation subgroup of order n (Dornberger-Schiff, 1964, 1966; Ďurovič, 1994b). The basis vectors of a superposition structure are called *superposition vectors*: they are obtained by completing the partial symmetry operations of a space groupoid to total symmetry operations of a space group (Fichtner, 1977).

Among the possible superposition structures, the one in which all the possible positions of all OD layers are simultaneously realized is called family structure (Ďurovič, 1994b). All the diffractions corresponding to the family structure are sharp and common to all the members of the family and are called *family reflections* (or *family diffractions).* The remaining ones are called *non-family reflections* and are typical of each polytype; they can be sharp or diffuse, depending whether the polytype is ordered or not (Ďurovič, 1992, 1997, Ďurovič and Weiss, 1986).

Within Pauling model, the family structure is a 9-fold superposition structure that corresponds to superpositions $\pm a/3$ and $\pm b/3$; its symmetry is $P(6/m)mm$ (Dornberger-Schiff *et al*, 1982). To any of the atoms in the layer, eight additional atoms are generated in the family

[*3] OD stands for "Order-Disorder". However, OD phenomena are of completely different nature from the order-disorder phenomena in alloys.

structure, with coordinates ($x\pm1/3$, y); (x, $y\pm1/3$) and ($x\pm1/3$, $y\pm1/3$). The family reflections are those with h = 0(mod 3) and k = 0(mod 3) and the subgroup of translation has order 9. Since the layer stagger is $|a|/3$, the superposition vectors of Pauling model ($\pm a/3$ and $\pm b/3$) complete the partial symmetry operations of space groupoids to total symmetry operations of space groups after one single layer. Therefore, the period along c axis of the family structure is $c_0 = 1/c^*_1 = c_{1M}\sin\beta_{1M}$ and corresponds to the vertical distance between two closest interlayer cations. The basis vectors of the family structure are $A_1 = a_1/3$, $A_2 = a_2/3$, $C = c_0$ (Backhaus and Ďurovič, 1984; Ďurovič *et al.*, 1984; Ďurovič, 1994b).

Within the trigonal model two *subfamilies, A* and *B*, and thus two OD groupoid families exist. In subfamily A polytypes, next layers are rotated by $2n60°$ and the coordination polyhedra for the interlayer cations are trigonal antiprisms; the symmetry of the tetrahedral OD layer is $P(\bar{3})1m$. In subfamily B polytypes, next layers are rotated by $(2n+1)60°$ and the coordination polyhedra for the interlayer cations are trigonal prisms; the symmetry of the tetrahedral OD layer is $P(\bar{6})2m$. For both subfamilies the family structure is a 3-fold superposition structure and corresponds to superpositions $\pm b/3$. To any of the atoms in the layer, two additional atoms are generated in the family structure, with coordinates (x, $y\pm1/3$). The family reflections are those with k = 0(mod 3) and the subgroup of translation has order 3. The superposition vectors ($\pm b/3$) complete the partial symmetry operations of space groupoids to total symmetry operations of space groups after three layers in case of subfamily A, but after two layers in case of subfamily B. The basis vectors for the family structure are thus $A_1 = (a_1+2a_2)$, $A_2 = -(2a_1+a_2)$, C. For subfamily A, $C = 3c_0$; for subfamily B $C = 2c_0$. The symmetry of the family structure is $H_R3\bar{1}m$ (where the subscript R indicates that the smaller cell is rhombohedral) for subfamily A, and $H6_3/mcm$ for subfamily B (Ďurovič, 1994b). The adoption of the H-centred cell permit to describe the family structures and the real structures in the same axes, but additional absences appear in the diffraction pattern (Smrčok *et al.*, 1994).

Under the trigonal model, a third kind of mica polytypes exists, in which rotations by both $2n60°$ and $(2n+1)60°$ appear. These polytypes are called *mixed-rotation polytypes* (S. Ďurovič, personal communication) and contain both kinds of interlayer coordination polyhedra, violating the *VC*. It follows that they are non-OD polytypes, unless the ditrigonal rotation angle is zero. A few examples of them are known (for a short review see Nespolo, 1998) but the limited accuracy of the refinements does not give information on the angle of ditrigonal rotation.

The family reflections of the 9-fold family structure are common to all polytypes of the same mineral group (Zvyagin, 1967; Ďurovič, 1994b) and are thus not useful for the purpose of distinguishing individual polytypes. On the other hand, as shown below, reflections corresponding to $h \neq 0$(mod 3) and k = 0(mod 3) (family reflections of the 3-fold family structure) permit to distinguish whether a polytype belongs to subfamily A or B or it is a mixed-rotation polytype.

The examination of the family reflections and of the non-family reflections belonging to ($0kl$) plane, which are common to all polytypes with the same projection on the (b, c) plane, are usually enough to identify any polytype, except homometric structures (Weiss and Wiewióra, 1986; Ďurovič, 1992). However, due to the large number of possible stacking sequences, the solution of the stacking sequence of long period polytypes can be strongly challenging. The

analysis of the periodicity of the intensity distribution (Takeda, 1967; Sadanaga and Takeda, 1969; Takeda and Sadanaga, 1969; Takeda and Ross, 1995; Nespolo *et al.*, 1999b) for non-family reflections represents the most suitable and powerful tool to solve the stacking sequence of mica polytypes. However, in order to apply this method, the presence of twinning has to be excluded. Hereafter, general criteria to confirm or exclude the presence of twinning by reticular pseudo-merohedry are derived.

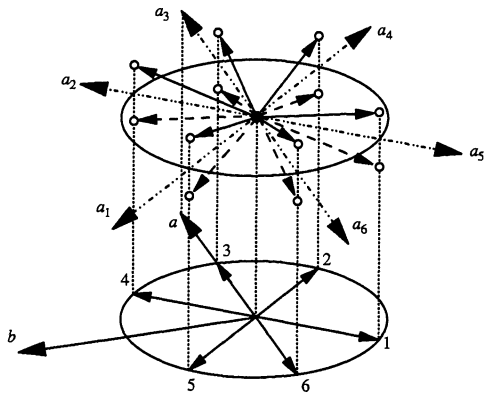

FIG. 4. Perspective view showing the intralayer displacements for micas with the origin of the *O* sheet in the M_1 site. White circles: interlayer cations. Small black circle: octahedral M_1 site, where the centre of symmetry and the origin of the space-fixed reference are located. Axes a_1-a_6 are structure-related orthohexagonal axes (b_1-b_6 axes, not shown, are perpendicular to the corresponding *a* axes). Z vectors are twice the vectors shown in the basal projection. The higher circle passes on the intersection points of the a_1-a_6 axes with the segment of perpendicular line connecting two interlayer cations.

5. Symbolic Description of Mica Polytypes.

Several symbolic descriptions of mica polytypes have been proposed by different authors. For the purposes of the present research, a space-fixed reference is needed, and descriptive symbols linked to it are the most suitable ones. These requirements are fulfilled by the symbols developed by Zvyagin and co-workers (Zvyagin *et al.*, 1979, Zvyagin, 1985; Zhukhlistov *et al.*, 1990), hereafter labelled Z *symbols*, which give the absolute orientations and the relative displacements of mica half-layers and are linked to the C_1 setting (Fig. 4). Looking at the sequence of layers always in the same direction, the vector connecting the origin of the *O* sheet with the nearest interlayer site and vice versa is called *intralayer displacement*. Its projection on the (001) plane has length $|a|/3$. Mica polytypes are obtained by stacking the M layer rotated by $n60°$ ($0 \leq n \leq 5$) and shifted along *c* (Smith and Yoder, 1956). There are thus six possible orientations for the M layer, indicated by the six structure-related a_i axes (i = 1-6). The projection of the intralayer displacement is indicated by the Z symbol i (i = 1,2,...6) when the a_i axis is parallel to the space-fixed axis *a* (Fig. 4) (Zvyagin, 1967; Zhukhlistov *et al.*, 1990). Since Z symbols are oriented symbols, their parity (odd or even) is commonly called *orientation parity* (Zvyagin, 1997). The (*a*, *b*) components (s_x, s_y) of intralayer displacements are given in Table 3. The total displacement vector for each layer (Z *vectors*, hereafter) is finally obtained by taking

TABLE 3. Z symbols and (*a*, *b*) components of the corresponding intralayer vectors in the C_1 setting. s_x and s_y are expressed as multiples of 1/3.

Z symbol	(s_x, s_y)
3	(1, 0)
4	(-1, -1)
5	(1, -1)
6	(-1, 0)
1	(1, 1)
2	(-1, 1)

twice the intralayer vectors*4; their (*a, b*) components are ($2s_x$, $2s_y$) (Table 3). Then, since ±2/3 is translationally equivalent to ∓1/3, in practice the (*a, b*) components of the Z vectors are the same as those of the intralayer displacements, but with the signs exchanged.

The projection $\mathbf{c}_n$ is translationally equivalent to (0, 0) (orthogonal polytypes), (±1/3, [0, ±1/3]) (*Class a* polytypes) and (0, ±1/3) (*Class b* polytypes). The correct space orientation of the structural model is obtained by rotating it around the normal to (001) until $\mathbf{c}_n$ = ($1\bar{}/3$, 0) (*Class a*) and $\mathbf{c}_n$ = (0,$\bar{1}$/3) (*Class b*). However, three and six orientations exist respectively for orthogonal and *Class b* polytypes that correspond to the same $\mathbf{c}_n$. They are equivalent for hexagonal, trigonal and triclinic polytypes but not for orthorhombic and monoclinic ones. The correct orientation can be evaluated taking into account the transformation rules between Z symbols (Zvyagin, 1974, 1997). In other words, the (*a, b*) components of $\mathbf{c}_n$ projection are sufficient to judge the correctness of the structural model orientation only in case of *Class a* polytypes (Nespolo *et al.*, 1999b); however, they allow to establish in a simple way the rules relating the subfamily on one hand, and the *Class* and *Subclass* on the other hand. The (*a, b*) components of the $\mathbf{c}_n$ projection of an *N*-layer polytype with respect to the space-fixed reference are simply obtained by summing the (*a, b*) components of the Z vectors corresponding to the *N* layers. The following relations are easily established.

Subfamily A: Successive layers are related by $2n60°$ rotations only and thus they have the same orientation parity; the *x* component of each stacking vector is either always -1/3 (odd orientation parity) or always +1/3 (even orientation parity). As a consequence, in *Series* 0 [n = 0 in Eq. (1), *i.e.* polytypes with a number of layers not multiple of 3] the *x* component cannot be 0 and these polytypes all belong to *Class a*. Furthermore, *Subclass* 1 polytypes have $3K$+1 layers and the *x* component of $\mathbf{c}_n$ is -1/3 only if the layers have all odd orientation parity. On the other hand, *Subclass* 2 polytypes have $3K$+2 layers and the *x* component of $\mathbf{c}_n$ is -1/3 only if the layers have all even orientation parity. In *Series* higher than 0 the number of layers building the polytypes is multiple of 3 and thus the *x* component of $\mathbf{c}_n$ is always 0. Therefore, these polytypes either are orthogonal or belong to *Class b*.

Subfamily B: Successive layers are related by $(2n+1)60°$ rotations only and thus they have alternating orientation parity. Only polytypes with an even number of layers appear in this subfamily. Besides, since layers with different orientation parity have opposite *x* component of the $\mathbf{c}_n$ projection, it is never possible to have a *Class a* polytype.

Mixed-rotation polytypes: Since there is no definite rule for the layer orientation parity sequence, in this case all the three kinds of polytypes (orthogonal, *Class a, Class b*) are possible.

Most of polytypes reported to date belong to subfamily A and, with few exceptions, they belong to *Series* 0: they are thus *Class a* polytypes. Two homogeneous subfamily B polytypes have been reported: $2M_2$ polytype (*Series* 0 *Class b*) occurs with a relatively high frequency in lithium micas; $2O$ polytype (orthogonal) was found only twice, in the brittle mica anandite (Giuseppetti and Tadini, 1972; Filut *et al.*, 1985). Only a few examples of

*4 This relation is valid within the so-called *homo-octahedral approximation*, in which the origin of the *O* sheet is always at the *M*1 site (Nespolo *et al.*, 1999b), but is not correct for the rare micas built by layers with the origin of the *O* sheet in one of the cis-coordinated sites, which are not considered here.

mixed rotation polytypes have been found (a short review is in Nespolo, 1998).

6. Reflection Conditions

In the diffraction pattern of mica polytypes, systematic absences extensively appear besides those due to the space group, which correspond to the *additional reflection conditions* (Hahn and Vos, 1996). The number and positions of reflections along the reciprocal lattice rows corresponding to the family reflections (hereafter called *family rows*, for shortness) of the 3-fold family structure permit to identify whether a mica polytype is OD or not, and to which of the two subfamilies an OD polytype belongs. Besides, they are particularly useful in evaluating the possible presence of twins. With this purpose, the reflection conditions for family rows are here analytically derived. A straightforward way to obtain them is by writing the structure factor by means of Zvyagin's functions A_j (j = 1-6), which represent the layer Fourier transform in the six possible orientations. These functions are expressed in the ortho-hexagonal cell of the C_1 setting and have the origin in the $M1$ site (Zvyagin, 1967). The structure factor can be written as (Nespolo and Kogure, 1998):

$$F(hkl)=\{\sum_{m=0}^{N'-1}A_m(hkl)\exp 2\pi i[hu_x(m)+ku_y(m)+lu_z(m)]\}\exp 2\pi i(hx_0+ky_0) \qquad (2)$$

where:

$$\begin{aligned} A(hkl)&=\sum_{j=1}^{n}f_j\cos 2\pi[hx_{i_m}(N',j,0)+ky_{i_m}(N',j,0)+lz(N',j,0)]= \\ &=\sum_{j=1}^{n}f_j\cos 2\pi[h_m x_3(N',j,0)+k_m y_3(N',j,0)+lz(N',j,0)]=A_3(h_m k_m l) \end{aligned} \qquad (3)$$

$$\begin{bmatrix} x_{im}(N',j,0) \\ y_{im}(N',j,0) \end{bmatrix}=\mathbf{U}_{3\to m}^{-1}\begin{bmatrix} x_3(N',j,0) \\ y_3(N',j,0) \end{bmatrix}$$
$$(h_m \;\; k_m)=(h_3 \;\; k_3)\mathbf{U}_{3\to m} \qquad (4)$$

$$\boldsymbol{u}_z(m)=m/N'. \qquad (5)$$

According to Arnold (1996), covariant and contravariant components are written as row matrices and column matrices respectively. $\mathbf{U}_{3\to m}$ is the rotation matrix transforming a layer in orientation 3 into a layer in orientation i_m [see Table 1 in Takeda (1967)], where i_m is the Z symbol (1-6) of the *m-th* layer (m = 0, N'-1). $x_{i_m}(N',j,0)$, $y_{i_m}(N',j,0)$ and $z(N',j,0)$ are the *x, y, z* fractional coordinates of the *j-th* atom inside the first layer (m = 0), assumed in orientation i_m (z is not affected by the layer orientation). $u_x(m)$, $u_y(m)$ and $u_z(m)$ are the *x, y, z* components of the stacking vector leading from the origin of the first layer to the origin of the *m-th* one. x_0 and y_0 are the coordinates of the whole structure with respect to the origin of the first layer and are non-zero only for non-centrosymmetric structures with a preferred origin: the only polytype having this feature reported to date is 3*T*, for which x_0 = 0, y_0 = ±1/9 (Zvyagin, 1967; Nespolo and Kogure, 1998). 6*H* polytype is another example, but it has never been reported. h_m and k_m indices as a function of h_3 and k_3 are given in Table 4.

In Eq. (3) the atomic coordinates depend upon the model chosen to describe mica layer. The Pauling model and the trigonal model differ only for the ditrigonal rotation, *i.e.* in the

TABLE 4. h_m and k_m indices expressed as function of h_3 and k_3, the *h, k* Miller indices for a layer in orientation Z = 3

m	h_m	k_m
3	h_3	k_3
4	$(h_3+k_3)/2$	$(-3h_3+k_3)/2$
5	$(-h_3+k_3)/2$	$-(3h_3+k_3)/2$
6	$-h_3$	$-k_3$
1	$-(h_3+k_3)/2$	$(3h_3-k_3)/2$
2	$(h_3-k_3)/2$	$(3h_3+k_3)/2$

coordinates of the basal oxygen atoms. The more the ditrigonal rotation is marked, the more the intensities computed according to the two models differ. However, the reflections conditions are not significantly influenced by the ditrigonal rotation, and the appearance of weak reflections violating the reflection conditions is mainly due to the vacancy in one of the octahedral sites of dioctahedral micas, and to the consequent distortions in the *O* sheet (Rieder, 1968). Therefore, the reflection conditions can be derived even applying the simplest Pauling model. The adoption of the trigonal model in practice does not modify the reflection conditions, but it changes the definition of family reflections, and thus the interpretation of the diffraction pattern.

Labelling z_{O_B} the z coordinate of basal oxygen atoms, z_{OH} that of hydroxyls and of apical oxygen atoms, and inserting the atomic coordinates according to Pauling model (Zvyagin, 1967), the A_3 function can be written as (Nespolo and Kogure, 1998):

$$\begin{aligned} A_3(h_m k_m l) = {} & f_{M_1} + 2f_{M_2}\cos 2\pi k_m/3 + f_I \cos 2\pi(h_m/3 + l/2N') + \\ & + 2f_0(1+2\cos 2\pi k_m/3)\cos 2\pi(h_m/3 + lz_{OH}/N') + \\ & + 4f_T \cos 2\pi(h_m/3 + lz_T/N')\cos 2\pi k_m/3 + \\ & + 2f_0[\cos 2\pi(-h_m/6 + lz_{O_B}/N') + 2\cos 2\pi(h_m/12 + lz_{O_B}/N')\cos 2\pi k_m/4] \end{aligned} \qquad (6)$$

Peculiarities of the cation composition are in the atomic scattering factor. $4f_T$ is a short notation that depends upon the actual occupation of *T* sites; f_I represents the atomic scattering factor of the interlayer cations. In Eq. (2) u_x and u_y are obtained in the following way. The origin of each layer is at the *M*1 site, *i.e.* in the middle point of the corresponding Z vector. The origin shift from the first to the *p-th* layer is obtained through summation of the *x, y* coordinates of the first and the *p-th intralayer* displacement vectors (s_x, s_y) and those of the Z vectors connecting them ($2s_x$, $2s_y$) (Table 3; Fig. 5). *p* is a running index that for orthogonal polytypes takes the integral values from 2 to *N*, while for non-orthogonal polytypes it takes the integral values from 2 to 3*N*. u_x and u_y are given by Eq. (7) and the result is expressed as 0, ±1/3 for both u_x and u_y by adding the *C*-centring vector (1/2, 1/2) when necessary

$$[u_x(p), u_y(p)] = [s_x(1), s_y(1)] + [s_x(p), s_y(p)] + \sum_{j=2}^{p-1} [2s_x(j), 2s_y(j)]. \qquad (7)$$

The ideal reflection conditions are obtained by looking for systematically repeated zero values of *F(hkl)* in Eq. (2). By introducing three functions (g_1, g_2 and g_3: see Table 5) of h_m and k_m, defined by substituting in Eq. (6) h_m and k_m from Table 4, Eq. (6) can be rearranged in a more suitable form:

$$\begin{aligned} A_3[g_1(h_m k_m), g_2(h_m k_m), g_3(h_m k_m), l] = {} & f_{M1} + f_{M2} 2\cos\pi(g_1) + f_I \cos 2\pi(g_2 + l/2N') + \\ & + 2f_o(1+2\cos g_1\pi)\cos 2\pi(g_2 + lz_{OH}/N') + 4f_T \cos 2\pi(g_2 + lz_T/N')\cos(g_1)\pi + \\ & + 2f_o \cos 2\pi(-g_2/2 + lz_{OB}/N') + 2\cos 2\pi(g_2/4 + lz_{O_B}/N')\cos(g_3)\pi \end{aligned} \qquad (6')$$

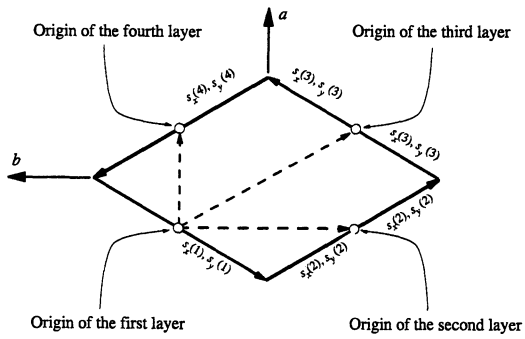

FIG. 5. Calculation of the components (u_x, u_y) of the vectors connecting the origin of the first layer with the origin of the next layers. s_x(j), s_y(j) are the (*a*, *b*) components of the j-th intralayer displacements (Table 3). Polytype $4O_4$ (Z=1245) is taken as example.

TABLE 5. g_1, g_2 and g_3 (Eq. 6') as functions of h_3 and k_3, the *h*, *k* Miller indices for a layer in orientation Z = 3.

Z	3	4	5	6	1	2
g_1	$2k_3/3$	$-h_3+k_3/3$	$-h_3-k_3/3$	$-2k_3/3$	$h_3-k_3/3$	$h_3+k_3/3$
g_2	$h_3/3$	$(h_3+k_3)/6$	$(-h_3+k_3)/6$	$-h_3/3$	$-(h_3+k_3)/6$	$(h_3-k_3)/6$
g_3	$k_3/2$	$(-3h_3+k_3)/4$	$-(3h_3+k_3)/4$	$-k_3/2$	$(3h_3-k_3)/4$	$(3h_3+k_3)/4$

Taking into account the C-centring condition $h+k = 0(\mathrm{mod}\ 2)$, it is easy to verify that, when $k = 0(\mathrm{mod}\ 3)$ (*i.e.* the family reflections of the 3-fold family structure), each of the seven terms in Eq. (6') takes the same absolute value independently from *m*; on the other hand, the sign depends upon the parity of *m*. It follows that (see also Zhukhlistov *et al.*, 1990; Zvyagin, 1997):

$$(A_3=A_1=A_5)=A\neq(A_6=A_4=A_2)=A' \quad [k = 0(\mathrm{mod}\ 3)] \qquad (8)$$

The isomorphous substitutions and the cation ordering in the octahedral sheet (Pavese *et al.*, 1997) modify the *F* value but do not invalidate Eq. (8). Besides, the ditrigonal rotation described by the trigonal model lowers the symmetry of the tetrahedral sheets from hexagonal to trigonal; this, again, has no effect on Eq. (8), since the identities stated by it regard A_m function related by $2n60°$ rotations. The reflection conditions however differ in the two subfamilies, since the relative disposition of layers differs.

Subfamily A polytypes are built by layers all with the same orientation parity. Therefore, Eq. (2) expressed for the family reflections only becomes:

$$F(hkl)=\{A(h_3k_3l)\sum_{m=0}^{N'-1}\exp 2\pi i[hu_x(m)+ku_y(m)+lu_z(m)]\}\exp 2\pi i(hx_0+ky_0) \qquad (2A)$$

Subfamily B polytypes are built by layers all with alternating orientation parity. Only polytypes with an even number of layers belong to this subfamily and Eq. (2) can be separated into two terms:

$$F(hkl)=\left\{\begin{array}{l} A\,(h_3k_3l)\sum_{m=0}^{N'-1}\exp 2\pi i[hu_x(m)+ku_y(m)+lu_z(m)]+ \\ +A'(h_3k_3l)\sum_{m=0}^{N'-1}\exp 2\pi i[hu_x(m')+ku_y(m')+lu_z(m')] \end{array}\right\}\exp 2\pi i\,(hx_0+ky_0) \qquad (2B)$$

where *m* corresponds to layers in odd orientation and *m'* to layers in even orientation [A and A' are given in Eq. (8)].

No similar simplification is in general possible for mixed-rotation polytypes, since the orientation parity of layers does not follow a precise rule.

The reflection conditions in the two subfamilies are derived in the Appendix, where the exponential term including (x_0, y_0) is neglected. Taking into account that for non-orthogonal

polytypes only one out of three of the orthogonal l indices corresponds to integer monoclinic indices, the following conclusions are obtained:

1. along family rows with $h = 0(\text{mod } 3)$ (family rows of the 9-fold family structure) one reflection out of N always appears;
2. along family rows with $h \neq 0(\text{mod } 3)$ (family rows of the 3-fold family structure) one reflection out of N appears in case of subfamily A, but two equally spaced reflections out of N appear in case of subfamily B;
3. for mixed-rotation polytypes, rows with $h \neq 0(\text{mod } 3)$ are non-family rows and in general they show N reflections, some of which may be absent.

7. Family Reflections and Axial Settings.

Let us now consider the reciprocal superlattice built on the family reflections only. Family reflections with both h and $k = 0(\text{mod } 3)$ correspond to the 9-fold family structure, whose period along c is c_0. On the other hand, family reflections with $h \neq 0(\text{mod } 3)$ and $k = 0(\text{mod } 3)$ correspond to the 3-fold family structure; for it the period along c axis is $3c_0$ (subfamily A) or $2c_0$ (subfamily B). However, the family structure of subfamily A polytypes admits a primitive rhombohedral cell, and only one reflection appears in the c^*_1 repeat. The a^* and b^* axes of C_1 setting are common to all polytypes. Expressing the l index in the c^*_1 period, one reflection appears along family rows of the 9-fold family structure, but one, two and N reflections along the family rows of the 3-fold family structure only [$h \neq 0$ (mod 3), $k = 0$ (mod 3)] for subfamily A, subfamily B and mixed-rotation polytypes respectively.

The adoption of a suitable axial setting makes easier to match the appearance of the family reflections in the diffraction pattern of different polytypes. All the polytypes belonging to the same *Series* and the same *Class* can be indexed in a particular axial setting showing the same ideal angle as the conventional cell of the shortest-period polytype of that *Series*. This setting is called **Fixed-angle setting** and is easily obtained from ${}^a\mathbf{S}$ and ${}^b\mathbf{S}$. The choice of a common setting for polytypes belonging to different *Series* is geometrically not possible (Nespolo *et al.*, 1997a; 1998). All the polytypes belonging to the same *Series* have the same ideal monoclinic angle in this setting. For the two *Classes* it is symbolized by ${}^{3^n,a}\mathbf{F}$ and ${}^{3^n,b}\mathbf{F}$, which for *Series* 0 are shortened in ${}^a\mathbf{F}$ and ${}^b\mathbf{F}$ (Nespolo *et al.*, 1997a; 1998).

The l index of the node corresponding to the single reflection in the diffraction pattern of subfamily A polytypes is given in Eq. (A2) and (A4). The superlattice built on family reflections can be overlapped for *all* polytypes belonging to subfamily A only if it is rotated by 180° around the normal to the layer when comparing polytypes built by layers of opposite orientation parity (see Appendix) (Fig. 6). This is due to the fact that the rhombohedral primitive cell of the family structure for subfamily A polytypes is in the obverse setting for odd orientation parity of the layers, but in the reverse setting for even orientation parity (S. Ďurovič, personal communication). In *Series* 0 (to which belong most of the polytypes reported to date), all polytypes belonging to subfamily A are *Class a* polytypes. Polytypes belonging to *Subclass* 1 are always built by layers with odd orientation parity, whereas those belonging to *Subclass* 2 are

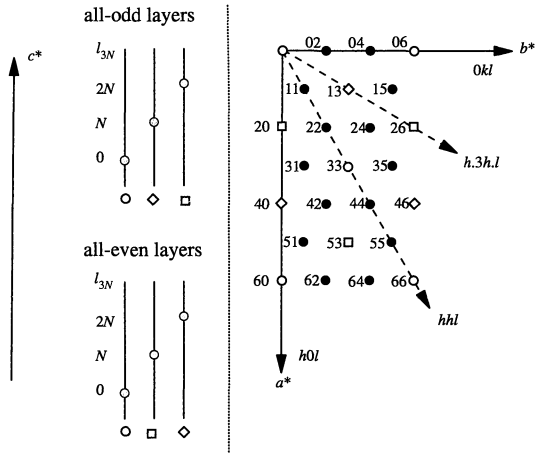

FIG. 6. Projection of the reciprocal lattice of subfamily A OD mica polytypes on the (a^*, b^*) plane (the independent portion in the monoclinic crystal system is shown). White marks: family reflections. Black dots: non-family reflections. l_{C_1} is the index of the family reflections in C_1 setting [Eq. (A2) and (A4) in the Appendix].

always built by layers with even orientation parity. The ^{a}**F** setting alternates the directions of (a, b) and (a^*, b^*) axes with the *Subclass* (Nespolo *et al.*, 1997b, 1998) and is exactly the axial setting leading to the overlap of the superlattice built on family reflections. In higher *Series*, polytypes belonging to subfamily A can be orthogonal or *Class b* polytypes and there is no longer a biunivocal correspondence. For example, the $3A_1$ (Z = 446) polytype[5] is a subfamily A *Series* 1 *Class b Subclass* 1 polytype described by layers with even orientation parity. The superlattice built on the family reflections of this polytype matches the superlattice built on the family reflections of $2M_1$ polytype (Z = 24), which is a subfamily A *Series* 0 *Class a Subclass* 2 (and thus described by layers with even orientation parity) polytype. The superlattice of both these polytypes obey the reflection condition $l_{C_1} = (2N'/3)h(\text{mod } N')$. The reciprocal superlattice built on family reflections of a polytype can be overlapped to the reciprocal superlattice of another polytype even belonging to another *Series*, but the orientation parity must be taken into account. Borutskiy *et al.* (1987) solved the stacking sequence of $3A_1$ polytype by means of the oblique-texture electron diffraction technique, in which reciprocal lattice rows parallel to c^* with the same value of $3h^2+k^2$ appear on one and the same ellipsis (Zvyagin, 1967), but they mistook the orientation parity, giving Z symbols as 113.

Subfamily B polytypes show one reflection out of N along family rows of the 9-fold family structure, but two along those of the 3-fold family structure. However, polytypes of this subfamily either are orthogonal or belong to *Class b*, for which the non-right angle is α (before the axes exchange) and the l_{C_1} index of the superlattice nodes does not depend on h (Eq. A6 in the Appendix). The reciprocal superlattice in this case matches for all polytypes (Fig. 7), which is consistent with the fact that the primitive cell of the family structure is hexagonal.

In mixed-rotation polytypes the family reflections are only those of the 9-fold family structure. Reflections corresponding to $h \neq 0(\text{mod } 3)$ and $k = 0(\text{mod } 3)$ are non-family reflections

*[5] According to the indications of the IUCr *Ad-Hoc* committee (Guinier *et al.*, 1984), lattice symbol for triclinic polytypes should be changed from *Tc* to *A* (Anorthic).

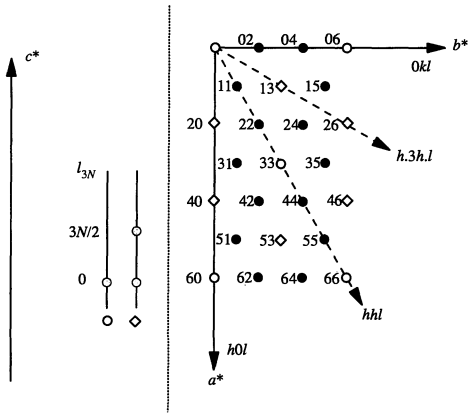

FIG. 7. Projection of the reciprocal lattice of subfamily B OD mica polytypes on the (a^*, b^*) plane. Symbols: same as in FIG. 6.

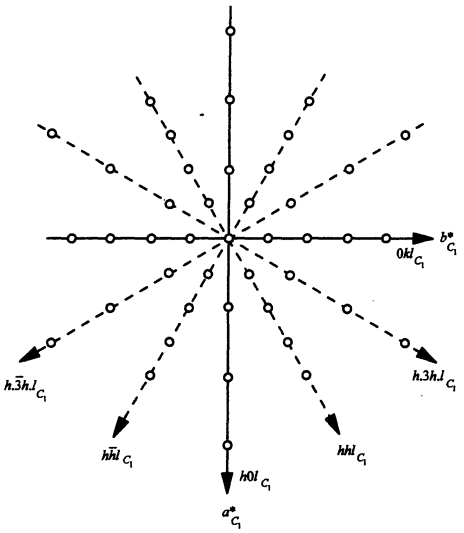

FIG. 8. Central planes usually observed by photographic techniques, in projection on (a^*, b^*) plane. Indexing in C_1 setting. The white marks simply define the positions of reciprocal lattice rows and do not convey information on l indices.

and they are influenced by the additional reflection conditions not in an unique way. However, these rows again convey important information, since their different appearance from those of polytypes belonging to the two subfamilies is indicative of mixed-rotation polytypes (see the examples in Kogure and Nespolo, 1999a,b).

8. Non-Family Reflections and Orthogonal Planes.

Once the kind of polytype (subfamily A, subfamily B or mixed-rotation) has been determined by analyzing the family reflections, the analysis of the intensity distribution along non-family rows allows the identification of the polytype, in case of single crystal. An ideal example of a diffraction pattern taken with a photographic technique, such as precession camera, is useful to illustrate the procedure. The crystal should be mounted as to have c^* coincident with the dial axis, so that c^* appears in all the photographs. Fig. 8 shows the six central planes which can be normally photographed by this technique, projected onto the (a^*, b^*) plane. These planes are divided into two groups, differing for the perpendicular separation between neighboring reciprocal lattice rows parallel to c^*. One group consists of planes $0kl$, hhl and $h\bar{h}\,l$: the separation between next reciprocal lattice rows is about 0.22Å^{-1}, *i.e.* about 4.6Å in direct space: it corresponds to d_{020}, ideally equal to d_{110}; in the following it will be indicated as d_1, for shortness. These planes contain non-family rows for $k \neq 0$(mod 3) and correspond to the first, third, fifth, eighth... ellipses in the practice of oblique-texture electron diffraction (Zvyagin, 1967). The second group consists of planes $h0l$, $h.3h.l$ and $h.\bar{3}$ $h.l$: the separation between reciprocal lattice rows is about 0.38Å^{-1}, *i.e.* about 2.6Å in direct

space: it corresponds to d_{200}, ideally equal to d_{130}: in the following it will be indicated as d_2, for shortness. For both subfamilies, these planes contain family rows only, whereas rows with $h \neq 0(\text{mod } 3)$ are non-family rows for mixed-rotation polytypes. This second group of planes correspond to the second, sixth, twelfth... ellipses (Zvyagin, 1967).

The planes corresponding to d_2 permit to identify whether a polytype belongs to subfamily A, subfamily B or it is a mixed-rotation polytype. Then, from the intensities measured along one or more non-family rows in the planes corresponding to d_1, the Periodic Intensity Distribution (PID) (Takeda, 1967; Sadanaga and Takeda, 1969; Takeda and Sadanaga, 1969; Takeda and Ross, 1995; Nespolo *et al*, 1999b) can be derived. PID corresponds to the Fourier transform of the stacking sequence and is obtained by removing from the structure factor the effect of the modulation by the single-layer Fourier transform:

$$S^N(\mathbf{h}) = \frac{G^N(\mathbf{h})}{G_0(\mathbf{h})} \approx \sum_{j=1}^{N} \exp 2\pi i(\mathbf{h} \cdot \mathbf{t}_j) \tag{9}$$

where S^N is the PID for an N-layer polytype, G^N is the polytype Fourier transform, G_0 the Fourier transform of the single layer, $\mathbf{h} = h,k,l$ and $\mathbf{t}_j$ is the j-th stacking vector. Comparison of observed and calculated PID values uniquely identifies the stacking sequence. However, the presence of twinning must be clearly excluded before applying PID and for this purpose the analysis of the geometry of the diffraction pattern is of primary importance (Nespolo and Takeda, 1999). For the practical purpose of interpreting the diffraction pattern, hereafter a plane is said to be orthogonal if it has an *orthogonal appearance*, *i.e.* if a reflection corresponding to $l_{C_1} = 0$ (family rows) or $l_{C_1} = 0(\text{mod } 3N)$ (non-family rows) appears on each row parallel to c^*. Since the $l_{C_1} = 0$ reflection on non-family rows may be weak or even absent, a different definition is given for the two kinds of rows. The number and features of the orthogonal planes depend both on the *Class* (lattice features) and on the subfamily (OD character). These are easily obtained by taking into account that subfamily B polytypes and subfamily A *Series* > 0 polytypes never belong to *Class a*, whereas subfamily A *Series* 0 polytypes always belong to *Class a*.

1. *Orthogonal polytypes* : In case of subfamily A polytypes, the three planes corresponding to d_1 only are orthogonal, according to the above definition. For subfamily B and mixed-rotation polytypes, all the six planes are orthogonal. 3*T* is the only orthogonal subfamily A polytype reported to date: it occurs with relatively high frequency. 2*O* polytype is the only orthogonal subfamily B polytype reported to date.
2. *Class a* polytypes: One orthogonal plane exists, which corresponds to d_1: it is (0*kl*).
3. *Class b* polytypes: No plane corresponding to d_1 can be orthogonal. In subfamily A polytypes (*Series* > 0) the family reflections for which $h \neq 0(\text{mod } 3)$ never correspond to $l_{C_1} = 0(\text{mod } 3)$ (Eq. A2 and A4 in the Appendix) and no orthogonal plane appears. In subfamily B, family reflections for which $h \neq 0(\text{mod } 3)$ show two reflections, one of which always corresponds to $l_{C_1} = 0(\text{mod } 3)$ (Eq. A6 in the Appendix): the three planes that correspond to d_2 are thus orthogonal. In mixed-rotation polytypes, rows for which $h \neq 0(\text{mod } 3)$ correspond to non-family reflections and on them in general N reflection appear. On

the basis of the relation between l indices in $^b\mathbf{T}$ and in C_1 settings ($l_{b_\mathbf{T}}$ and l_{C_1}; Table 1), the three planes corresponding to d_2 are orthogonal also in this case.

Attention should be paid to the indexing of subfamily A *Class b* polytypes, since they do not show any orthogonal plane (as defined above) in the diffraction pattern. This may sometimes become a possible source of confusion. For example, Ross *et al.* (1966) reported $3A_1$ polytype (Z=446) in a syderophillite sample, giving the angular parameters as α= 92°50', β= 94°58', γ= 90°. $3A_1$ is a subfamily A *Series* 1 *Class b* polytype: therefore, in $^b\mathbf{T}$ setting it has $\alpha > 90°$, $\beta=\gamma= 90°$. The angular parameters reported by Ross *et al.* (1966) correspond to the two angles between c^* and $[\bar{2}01]^*$ and between c^* and $[0\bar{2}1]^*$ respectively. On the basis of the linear cell parameters given by the authors, the correct angles are α= 95°43', $\beta=\gamma= 90°$, calculated by applying the law of direction cosines. The value of α has to be compared with the ideal value α = 95°53', obtained by the metric relations in Table 1.

9. Twin Laws for Mica Polytypes.

Due to the existence of pseudo-symmetries, micas can undergo twinning of more than one kind.

The most common twinning is by reticular pseudo-merohedry. It modifies the geometry of the diffraction pattern and its presence may be identified by careful inspection of the diffraction pattern itself. Reticular (pseudo)-merohedry twin elements are (pseudo)-symmetry elements belonging to a multiple lattice, which corresponds to a crystal system with higher symmetry than that to which the crystal belongs (Friedel, 1904); therefore both holohedral and merohedral crystals may undergo twinning by reticular (pseudo)-merohedry with the same twin laws.

In addition to these, merohedral crystals may undergo twinning by merohedry, the twin elements being the symmetry elements for the crystal lattice not contained in the crystal point group.

Finally, when the crystal lattice is close to a higher-symmetry crystal system, both holohedral and merohedral crystals may undergo twinning by pseudo-merohedry, the twin elements being the pseudo-symmetry elements for the higher-symmetry lattice not contained in the crystal point group. In micas this occurs for triclinic polytypes (both *Classes*), for *Class b* polytypes (both triclinic and monoclinic) and for metrically orthorhombic polytypes. Triclinic polytypes possess a pseudo-monoclinic conventional cell and thus both 2 and m may behave as twin elements by pseudo-merohedry, of which only one is independent in case of crystals belonging to point group $\bar{1}$. *Class b* polytypes admit a pseudo-rhombohedral primitive cell, and metrically orthogonal polytypes admit a pseudo-hexagonal primitive cell based on (a_1, a_2) axes.

The resulting twin elements for mica polytypes are shown in the following scheme, where the directions are given in the C_1 setting.

1. For metrically orthorhombic polytypes, four two-fold axes in the (001) plane, namely [110], $[1\bar{1}0]$, [310], $[3\bar{1}0]$, and the four planes quasi-normal to these axes, namely (130), $(1\bar{3}0)$, (110), $(1\bar{1}0)$, are pseudo-merohedry twin elements. They may give rise to *corresponding twins* as defined by Friedel (1904, 1926). For trigonal and hexagonal polytypes

twinning is by merohedry; however, depending upon the crystal class, some of the above elements may belong to the point group symmetry of the crystal; in such case they are no longer twin elements (Nespolo *et al.*, 1997a).

2. For *Class a* polytypes the twin lattice, based on C_1 cell, contains only the nodes belonging to one plane out of three. Twinning is by reticular pseudo-merohedry, with twin index 3. The twin elements are the four pairs given for orthorhombic polytypes, to which the two-fold axis along [100] and the reflection plane (100) (which are mutually perpendicular for metrically monoclinic polytypes) have to be added. For polytypes belonging to crystal class *m*, [010] is merohedry twin axis; for polytypes belonging to crystal class 2, (010) is merohedry twin plane. For triclinic polytypes, [010] and (010) are merohedry twin elements if the polytypes are metrically monoclinic; they are pseudo-merohedry twin elements otherwise. Of these, only one is independent if the crystal belongs to point group $\bar{1}$.
3. For *Class b* polytypes the pseudo-symmetry elements of the pseudo-rhombohedral primitive cell not contained in the crystal point group are pseudo-merohedry twin elements. They are the two axes [110] and [1$\bar{1}$0] and the two planes (130) and (1$\bar{3}$0). The symmetry elements of the lattice based on the C_1 cell not belonging either to the (pseudo)-monoclinic conventional cell or to the pseudo-rhombohedral primitive cell are reticular pseudo-merohedry twin elements. They are the three axes, [310], [3$\bar{1}$0] and [010], and the three planes (110), (1$\bar{1}$0) and (010), with the last axis and plane mutually perpendicular for metrically monoclinic polytypes. For polytypes belonging to crystal class *m*, [100] is merohedry twin axis; for polytypes belonging to crystal class 2, (100) is merohedry twin plane. For triclinic polytypes, [100] and (100) are merohedry twin elements if the polytypes are metrically monoclinic; they are pseudo-merohedry twin elements otherwise. Of these, only one is independent if the crystal belongs to point group $\bar{1}$.

The individuals of a mica twin related by the above listed twin elements are rotated each other by $n60°\pm2\varepsilon(0 \leq n \leq 5)$; ε depends upon the obliquity of the twin, but is small enough to be neglected for practical purposes (Donnay *et al.*, 1964; Nespolo *et al.*, 1997a,b). The relative rotation between two individuals twinned according to a given twin law is obtained by applying a symmetry or pseudo-symmetry operator of the structure to the corresponding twin operator. Results are shown in Table 6, where the relative rotations are given neglecting ε; the precise values, in which the factor $\pm2\varepsilon$ has to be included, are only slightly different.

TABLE 6. Relative rotations about the normal to the layer between mica twinned individuals (the angles shown are approximated by neglecting ε).

Twin operation	relative rotation		kind of twinning	
	Class a	*Class b*	*Class a*	*Class b*
$[3\bar{1}0]_\pi$ / (110)	240°	300°	Reticular pseudo-merohedry	Pseudo-merohedry
$[310]_\pi$ / (1$\bar{1}$0)	120°	60°	Reticular pseudo-merohedry	Pseudo-merohedry
$[110]_\pi$ / (1$\bar{3}$0)	300°	240°	Reticular pseudo-merohedry	Reticular pseudo-merohedry
$[1\bar{1}0]_\pi$ / (130)	60°	120°	Reticular pseudo-merohedry	Reticular pseudo-merohedry
$[100]_\pi$ / (100)	180°	0°	Reticular pseudo-merohedry	Merohedry#
$[010]_\pi$ / (010)	0°	180°	Merohedry#	Reticular pseudo-merohedry

#In metrically triclinic polytypes these twin operations correspond to pseudo-merohedry.

10. Diffraction Patterns from Twins.

The twin reciprocal lattice results from the overlap of the crystal reciprocal lattices (Buerger, 1954). Rows with different *h, k* in the crystal-fixed reference coalesce into a single twin row. For non-orthogonal polytypes the metric relations $l_{C_1} = h$ (mod 3) (*Class a*) and $l_{C_1} = k$ (mod 3) (*Class b*) hold (see Table 1). Depending upon the twin law(s) (and thus the relative orientation of twinned individuals), non-family reflections from different individuals may either overlap or take positions separated by $c^*_1/3N$, where N is the number of layers in the repeat unit (Table 1). When two of the three positions in a c^*_1/N repeat are occupied, the presence of twinning is immediately evident, because of the sequence of two present and one absent reflections. On the other hand, when all the three positions are occupied, the presence of twinning is not evident: in this case the number of reflections in a c^*_1 repeat of a non-orthogonal twinned N-layer polytype is the same as that of an untwinned $3N$-layer polytype (apparent polytypism; Takano and Takano, 1958). Therefore, when the number of reflections in a c^*_1 repeat is multiple of 3, the possible presence of twinning by reticular pseudo-merohedry has to be considered.

If twinning is not recognized, the PID analysis may in principle lead to accept a wrong stacking sequence. PID determines the stacking sequence by looking for the *best match* of the PID values derived from the measured intensities and those computed from the stacking sequence of all polytypes with the same number of layers. The quality of the match (R factor) depends first of all on the quality of the crystal and it is in general lower than for structure refinement. The PID computed from $3N$ reflections coming from three (or more) individuals still corresponds to a periodic function and its values depend upon the volume ratio of the twinned individuals. If they sufficiently match the PID computed from the stacking symbols of one of the $3N$-layer polytypes, the corresponding stacking sequence might be accepted as the correct one. Nespolo and Takeda (1999) have shown that the opposite case is also possible: assuming the presence of twinning where it is absent and computing PID from a subset of reflections, the diffraction pattern can be wrongly ascribed to a shorter-period polytype. The presence of twinning has thus to be carefully examined before applying PID analysis.

Twinning is not at all a rare phenomenon in micas, as shown by several twinned crystals described even in Goldschmidt's atlas (1918). The low number of diffractional studies of mica twins is perhaps due to the difficulties of distinguishing them from longer period polytypes. However, in most cases the presence of twinning by reticular pseudo-merohedry can be confirmed or excluded by a simple inspection of the geometry of the diffraction pattern.

Nespolo *et al.* (1997b) have shown that for 1*M* mica the twin operations lead to classify reciprocal lattice rows into three kinds, which are not mixed by the twin operations. In case of twinning by reticular (pseudo)-merohedry, since the twin lattice is based on the C_1 cell for all polytypes, the same classification holds in general. One of these three kinds of rows, called **D** (for "double"), corresponds to the family reflections of the 3-fold family structure only [$h \neq 0$ (mod 3), $k = 0$(mod 3)]. Twinning of non-orthogonal polytypes modifies the appearance of

these rows. The number and the position of reflections along these rows depend upon the number of layers and the kind of polytype (subfamily A, subfamily B, mixed-rotation) and have to be evaluated in the c^*_1 repeat.

1. Twinning of subfamily A polytypes in which individuals are rotated by $(2n+1)60°$ corresponds to twinning by reticular pseudo-merohedry. It produecs separation of the single reflection on **D** rows from each individual into two reflections, corresponding to $l(c^*_1) = 1(\text{mod } 3)$ and $l(c^*1) = 2(\text{mod } 3)$; no reflection appears corresponding to $l(c^*_1) = 0(\text{mod } 3)$; this pattern is clearly different from that of a subfamily B polytypes, where two equally spaced reflections appear. Besides, if rotation is by ±60°, for *Series* 0 polytypes (*Class a*) the orthogonal plane of one individual necessarily overlaps a non-orthogonal plane of another individual and in the resulting diffraction pattern two or three orthogonal planes appear, corresponding to d_1.
2. Twinning of subfamily A polytypes in which individuals are rotated by $2n60°$ corresponds to twinning by reticular pseudo-merohedry in case fo *Class a* (*Series* 0), but to pseudo-merohedry, in case of *Class b* (*Series* > 0). It produces overlap of the single reflection on **D** rows from each individual; no reflection appears corresponding to $l(c^*_1) = 0(\text{mod } 3)$. However, for *Series* 0 (*Class a*) polytypes this twinning produces two or three orthogonal planes corresponding to d_1. When three such planes appear (three or more twinned individuals), the geometrical features of the diffraction pattern are the same as for orthogonal *Series* 1 polytypes. This situation corresponds to the well known example of 3*T* polytype *vs.* twinned 1*M*, which - at least for dioctahedral micas - can be distinguished by careful examination of the appearance of weak reflections violating the reflection conditions (*e.g.* Nespolo and Kogure, 1998). If the twin involves only two individuals, next reflections along non-family rows are unequally separated (1/3 and 2/3) and two orthogonal planes corresponding to d_1 appear: the presence of twinning is thus easily recognized.
3. Subfamily B polytypes either are orthogonal or belong to *Class b*. In the second case only three of the five pairs of twin laws correspond to twinning by reticular pseudo-merohedry. However, the corresponding twin operations lead to the overlap of the two reflections on **D** rows from each individual; no orthogonal plane appears corresponding to d_1, whereas the three planes corresponding to d_2 are orthogonal. The presence of twinning is not evident.
4. For mixed-rotation polytypes D rows are non-family rows. For *Class a* polytypes, two individuals rotated by 180° share one and the same orthogonal plane (0*kl*), but reflections are unequally spaced. The presence of twinning is thus evident. In the other cases, two or more orthogonal planes appear corresponding to d_1, as for subfamily A polytypes of the same *Class*, but no orthogonal planes appear corresponding to d_2. The presence of twinning is again evident. For *Class b* polytypes the three planes corresponding to d_2 are orthogonal and the presence of twinning is not evident.

In Tables 7a-7c the complete scheme of the identification process is shown. The approximated relative rotations between twinned individuals are given: the corresponding twin laws are easily obtained from Table 6. For *Class a* polytypes (which represent most of the polytypes reported to date) the presence of twinning can be confirmed or excluded by

TABLE 7a. Classification of diffraction patterns for $N = 3K+L$ ($d_1 = d_{020} \approx d_{110}$; $d_2 = d_{200} \approx d_{130}$). For the correspondence between the relative rotations of twinned individuals and the twin laws see Table 6.

	Number of reflections in the c^*_1 repeat along reciprocal lattice rows corresponding to family reflections			
Noumber of planes with orthogonal appearance	1	2		N
	$[l_{C_1} \neq 0 (\text{mod } 3)]$	$l_{C_1} = 1 (\text{mod } 3)$ and $2 (\text{mod } 3)$	$l_{C_1} = 0 (\text{mod } N)$ and $N/2 (\text{mod } N)$	
$1(d_1)$	*Subfamily A* Series 0 *Class a* untwinned polytype	———	———	Mixed-rotation *Series* 0 *Class a* untwinned polytype
$3(d_1)$	*Subfamily A* Series 0 orthogonal polytype untwinned or ±120°-twinned	*Subfamily A Series* 0 orthogonal(±60° / 180°)-twinned polytype	———	———
$3(d_2)$	———	———	*Subfamily B Series* 0 *Class b* polytype untwinned or ±120°-twinned	Mixed-rotation *Series* 0 *Class b* polytype untwinned or ±120°-twinned
6 (both d_1 and d_2)	———	———	*Subfamily B Series* 0 orthogonal polytype	Mixed-rotation *Series* 0 orthogonal polytype

TABLE 7b. Classification of diffraction patterns for $N = 3(3K+L)$ ($d_1 = d_{020} \approx d_{110}$; $d_2 = d_{200} \approx d_{130}$). For the correspondence between the relative rotations of twinned individuals and the twin laws see Table 6.

	Number of reflections in the c^*_1 repeat along reciprocal lattice rows corresponding to family reflections			
Number of planes with orthogonal appearance	1	2		N
	$[l_{C_1} \neq 0 (\text{mod } 3)]$	$l_{C_1} = 1 (\text{mod } 3)$ and $2 (\text{mod } 3)$	$l_{C_1} = 0 (\text{mod } N)$ and $N/2 (\text{mod } N)$	
0	*Subfamily A Series* 1 *Class b* polytype untwinned or ±120° -twinned	———	———	———
$1(d_1)$	———	*Subfamily A Series* 0 *Class a* polytype 180°-twinned	———	Mixed-rotation *Class a: Series* 1 untwinned polytype; *Series* 0 polytype180°-twinned
$2(d_1)$	*Subfamily A Series* 0 *Class a* polytype ±120°-twinned (two individuals)	*Subfamily A Series* 0 *Class a* polytype ±60°-twinned (two individuals)	———	Mixed-rotation *Series* 0 *Class a* polytype (±60°/±120°) -twinned (two individuals)
$3(d_1)$	*Subfamily A Series* 0 *Class a* polytype ±120°-twinned (three individuals) *Subfamily A Series*1 orthogonal polytype untwinned ±120°-twinned	*Subfamily A Series* 0 *Class a* polytype ±60°-twinned (three individuals) *Subfamily A Series* 1 orthogonal polytype (±60°/±180°) -twinned	———	Mixed-rotation *Series* 0 *Class a* polytype (±60°/±120°) -twinned (three individuals)
$3(d_2)$	———	———	*Subfamily B Class b*: *Series* 1 polytype untwinned or ±120° -twinned *Series* 0 polytype (±60°/180°)-twinned	Mixed-rotation *Class b*:*Series* 1polytype untwinned or ±120° -twinned *Series* 0 polytype (±60°/ 180°)-twinned polytype
6 (both d_1 and d_2)	———	———	*Subfamily B Series* 1 orthogonal polytype	Mixed-rotation *Series* 1 orthogonal polytype

TABLE 7c. Classification of diffraction patterns for $N=3^{n>1}(3K+L)(d_1=d_{020}\approx d_{110}; d_2=d_{200}(d_{130})$. For the correspondence between the relative rotations of twinned individuals and the twin laws see TABLE 6.

	Number of reflections in the c^*_1 repeat along reciprocal lattice rows corresponding to family reflections			
Number of planes with orthogona appearance	1	2		N
	$[l_{C_1} \neq 0 \pmod 3]$	$l_{C_1} = 1 \pmod 3$ and $2 \pmod 3$	$l_{C_1} = 0 \pmod N$ and $N/2 \pmod N$	
0	*Subfamily A Series n Class b* polytype untwinned or ±120°-twinned	*Subfamily A Series n-1 Class b* polytype (±60°/180°)-twinned	———	———
$1(d_1)$	———	———	———	Mixed-rotation *Classa*: *Series n* polytype *n*-1 untwinned; *Series* polytype 180°-twinned
$2(d_1)$	———	———	———	Mixed-rotation *Series n-1 Class a* polytype (±60°/±120°)-twinned (two individuals)
$3(d_1)$	*Subfamily A Series n* orthogonal polytype untwinned or ±120° -twinned	*Subfamily A Series n* orthogonal polytype (±60° /180°)-twinned	———	Mixed-rotation *Series n-1Class a* polytype (±60°/±120°)-twinned (three individuals)
$3(d_2)$	———	———	*Subfamily B Class b*: *Series n* polytype untwinned or ±120° -twinned; *Series n*-1 (±60°/180°)-twinned polytype	Mixed-rotation *Class b*: *Series n* polytype untwinned or ±120° -twinned; *Series n*-1 (±60°/180°)-twinned polytype
6(both d_1 and d_2)	———	———	*Subfamily B Series n* orthogonal polytype	Mixed-rotation *Series n* orthogonal polytype

simple inspection of the geometry of the diffraction pattern. Special attention is however needed to distinguish a $3N$-layer orthogonal polytype from the spiral twinning of three (or more) non-orthogonal N-layer *Class a* polytypes in which the individuals are rotated by $2n60°$. For *Class b* subfamily A *Series* 1 polytypes the presence of reticular pseudo-merohedry twinning is also evident. In the other cases the presence of twinning cannot be confirmed or excluded by analyzing the geometry of the diffraction pattern.

11. Identification of the Stacking Sequence.

The procedure derived in the previous sections permits to confirm or exclude the presence of twinning for most common polytypes. In absence of twinning it is possible to identify the stacking sequence on an unknown polytype by analyzing the observed and computed values of the PID function. In principle, this comparison should be accomplished considering all the cyclic permutations and the inversion of the whole sequence of values, that means $2N$ comparisons for each possible stacking sequence of an N-layer polytype. However, by expressing both the computed values and the measured ones in the $^{(3^n,a;3^n,b)}\mathbf{F}$ settings, this necessity is removed and the number of cycles is thus reduced by the factor $1/(2N)$ (Nespolo *et al.*, 1998).

The number of reflections along reciprocal lattice rows with $h \neq 0 \pmod 3$ and $k = 0 \pmod$

3) unequivocally identified the kind of polytype (subfamily A: Z symbols of the same parity; subfamily B: Z symbols of alternating parity; mixed-rotation: Z symbols of mixed parity). The most common polytypes belong to subfamily A; no inhomogeneous subfamily B have been reported to date; mixed-rotation polytypes only rarely occur. The number of polytypes with a given number of layers is by far larger in case of mixed-rotation polytypes. For example, there are 254.721 possible polytypes with 10 layers in the repeat unit. Of these, 572, 580 and 253.569 are subfamily A, subfamily B and mixed-rotation polytypes respectively. Of the 5.094.420 (2×10×254.721) comparisons that in principle are needed, consideration of the family reflections separates these possibilities into 11.440, 11.600 and 5.071.380 respectively; indexing in the $^{(3^n,a;3^n,b)}\mathbf{F}$ settings further reduces these numbers to 572, 580 and 253.569 respectively. For a 10-layer subfamily A polytype only 572 comparisons are really necessary.

12. Twinning by Pseudo-Merohedry and Allotwinning.

Twinning by merohedry does not modify the geometry of the diffraction pattern and should be investigated on the basis of the intensity analysis. In case of micas, the same is true also for twinning by pseudo-merohedry, because of the small obliquity of the twin (Donnay *et al.*, 1964).

Twins by merohedry is subdivided into two classes (Catti and Ferraris, 1976). Class I includes twins for which the crystal Laue symmetry coincides with the lattice symmetry, and the twin operation belongs to the Laue symmetry of the crystal. The twin contains only two individuals, which are necessarily hemihedral crystals. Reflections related by the twin operation are equivalent under Friedel's law and the presence of twinning cannot be recognized, unless the crystal is not centrosymmetric and anomalous scattering is used. On the other hand, class II includes twins for which the crystal Laue symmetry is lower than the lattice symmetry. At least part of the reflections related by the twin operation(s) are not equivalent even under Friedel's law.

Twins of *Class b* mica polytypes in which the twin operations are (pseudo)-symmetry operations for the pseudo-rhombohedral primitive cell are class II twins, as defined by Catti and Ferraris (1976). Because of the very small obliquity of the twin (Donnay *et al.,* 1964), the presence of twinning cannot be recognized by inspection of the geometry of the diffraction pattern. The possible presence of this kind of twinning potentially hinders the application of PID analysis to the diffraction pattern of a *Class b* polytype, since the reflections related by the twin operations are non-equivalent. The measured PID (S^N_{meas}) is thus a function of the PID of the individuals (S^N_1, S^N_2,....). In case of two-individuals it can be written as (see Eq. 9):

$$I_{meas}(\mathbf{h})=I_1(\mathbf{h})+I_2(\mathbf{h})=K\cdot\{[G_1^N(\mathbf{h})]^2+[G_2^N(\mathbf{h})]^2\}=K\cdot\{[G_0(\mathbf{h})\cdot S_1^N(\mathbf{h})]^2+[G_0(\mathbf{h})\cdot S_2^N(\mathbf{h})]^2\}$$
$$S^N_{meas}(\mathbf{h})=\{[S^N_1(\mathbf{h})]^2+[S^N_2(\mathbf{h})]^2\}^{1/2} \qquad (10)$$

where K is constant including all the corrections factors (Lorentz, Polarization, Transmission, Extinction, Scale). For subfamily A polytypes PID takes the same values along all the

non-family rows in planes corresponding to d_1, but the origin of PID along these rows is a function of h and k; besides, rows related by $(2n+1)60°$ have an opposite sequence of the N values (Nespolo *et al.*, 1999b). It follows that in Eq. (9) $S_1^N(h_1k_1l_1)_{C_1} = S_2^N(h_2k_2l_2)_{C_1}$, where h_1k_1 and h_2k_2 are related by $\pm 120°$ rotations around the normal to the layer and $l_2 = l_1 + m$, m being an integer. The resulting $(S^N_{meas})^2$ is thus the sum of squares of two or more sequence of the same S^N but with a different origin along z. The probability that S^N_{meas} matches the values computed from the stacking sequence of a different subfamily A polytype is rather low and the lack of a good match should be taken as a "danger signal" for the presence of twinning.

More intriguing is the presence of allotwinning, *i.e.* the oriented crystal association of different polytypes (Nespolo *et al.*, 1999a). If two or more polytypes with the same number of layers and the same lattice symmetry are allotwinned, the S^N_{meas} is actually the composition of two or more *different* S^N and in principle it might sufficiently match the computed PID of a different polytype, again with the same number of layers and the same lattice symmetry. Further research is needed in order to develop general criteria to exclude the presence of allotwinning.

Appendix. Analytical derivation of the reflection conditions.

A.1 Subfamily A.

Having all the layers the same orientation parity, the $u_x(m)$ component corresponds to the sequence 0, -1, 1.... (all-odd layers) or 0, 1 -1 (all-even layers) (see Table 3); this regular alternation of the u_x component and the $k = 0(\mathrm{mod}\ 3)$ condition lead to simplify the exponential term in Eq. (2A). In order to mathematically treat in the same way both the orthogonal and the non-orthogonal polytypes, the number of layers in the unit cell of the C_1 setting (N') is here expressed as a function of an integer Q. Orthogonal polytypes appear only in *Series* higher than 0 (*i.e.* when the number of layers is multiple of 3): for them $N' = N = 3Q$. For non-orthogonal polytypes $N' = 3N = 3Q$ and thus $N = Q$; Eq. (2A) can be re-written as a function of Q, being valid for both orthogonal and non-orthogonal polytypes, since in both cases $N' = 3Q$. In the following, it will be shown that 1) for all polytypes belonging to this subfamily only, all but one reflections out of N are absent in all the rows parallel to c^* corresponding to *family reflections*; 2) the l index of the present reflection depends on h; 3) the relation between l and h is different for polytypes built by all-odd and by all-even layers.

A.1.1 All-odd layers.

Eq. (2A) can be suitably simplified by separating the two cases with even and odd number of layers.

1. $\boldsymbol{Q = 2M}$. The first exponential is 1 $[u_x(0)=u_z(0)=0]$ and the $(3Q/2)$-th one is $(-1)^l$ $(u_x=0: u_z=1/2)$. To the m-th term $(m \neq 0)$ *i.e.* $\exp 2\pi i[u_x(m)h+u_z(m)l]$, always corresponds the $(Q-m)$-th term, *i.e.* $\exp 2\pi i[-u_x(m)h-u_z(m)l]$ and the sum is simply $2\cos 2\pi[u_x(m)h+u_z(m)l]$. Only the first half of the sequence $(0 \leq m \leq 3Q/2$ *i.e.* the first $3Q/2+1$ terms) has to be taken into account. Eq. (2A) is thus simplified as follows:

$$F=A\left\{-1+(-1)^l+2\sum_{P=0}^{\frac{Q-2}{2}}\left[\cos 2\pi\frac{Pl}{Q}+\cos 2\pi\left[\frac{h}{3}-\frac{3P+1}{3Q}l\right]+\cos 2\pi\left[\frac{h}{3}+\frac{3P+2}{3Q}l\right]\right]\right\} \quad \text{(A1)}$$

where the -1 is due to the fact that $P = 0$ has been included also in the first cosine term (whose value is 2). Further simplification is obtained by considering the possible relations between l and Q.

a. For $l \neq 0(\text{mod } Q)$, Eq. (A1) can be simplified by means of well-known trigonometric transformation formulae.

$$\sum_{P=0}^{\frac{Q-2}{2}}\cos 2\pi\frac{Pl}{Q}=\frac{\sin\frac{Q}{2}\cdot\frac{\pi l}{Q}}{\sin\frac{\pi l}{Q}}\cos\frac{Q-2}{2}\cdot\frac{\pi}{Q}=\sin\frac{\pi l}{2}\cos\frac{\pi l}{2}\frac{\cos\frac{\pi l}{Q}}{\sin\frac{\pi l}{Q}}+\sin^2\frac{\pi l}{2}=\sin^2\frac{\pi l}{2}$$

$$\sum_{P=0}^{\frac{Q-2}{2}}\sin 2\pi\frac{Pl}{Q}=\frac{\sin\frac{Q}{2}\cdot\frac{\pi l}{Q}}{\sin\frac{\pi l}{Q}}\sin\frac{Q-2}{2}\cdot\frac{\pi}{Q}=\sin^2\frac{\pi l}{2}\frac{\cos\frac{\pi l}{N}}{\sin\frac{\pi l}{N}}-\sin\frac{\pi l}{2}\cos\frac{\pi l}{2}=\sin^2\frac{\pi l}{2}\frac{\cos\frac{\pi l}{Q}}{\sin\frac{\pi l}{Q}}$$

$$\sum_{P=0}^{\frac{Q-2}{2}}\left[\cos 2\pi\left(\frac{h}{3}-\frac{3P+1}{3Q}l\right)+\cos 2\pi\left(\frac{h}{3}+\frac{3P+2}{3Q}l\right)\right]=\sum_{P=0}^{\frac{Q-2}{2}}\left[2\cos\pi\left(\frac{2h}{3}+\frac{l}{3Q}\right)\cos\pi\left(\frac{2P+1}{3Q}\right)\right]=$$

$$=2\cos\pi\left(\frac{2h}{3}+\frac{l}{3Q}\right)\left[\cos\pi\frac{l}{Q}\sum_{P=0}^{\frac{Q-2}{2}}\cos 2\pi\frac{Pl}{Q}-\sin\pi\frac{l}{Q}\sum_{P=0}^{\frac{Q-2}{2}}\sin 2\pi\frac{Pl}{Q}\right]=\left(\frac{2h}{3}+\frac{l}{3Q}\right)\cdot 0=0$$

$$F=A\left\{-1+(-1)^l+2\sin^2\frac{\pi l}{2}\right\}$$

and thus:

$l = 2n$: $F = A(-1 + 1 + 0) = 0$

$l = 2n\text{-}1$: $F = A(-1 -1 +2) = 0$

b. $l = Q(\text{mod } 3Q)$.

$$F=2A\sum_{P=0}^{\frac{Q-2}{2}}\left[\cos 2\pi P+\cos 2\pi\left(\frac{h}{3}-\frac{3P+1}{3}\right)+\cos 2\pi\left(\frac{h}{3}+\frac{3P+2}{3}\right)\right]=$$

$$=2A\left[1+\cos 2\pi\left(\frac{h-1}{3}\right)+\cos 2\pi\left(\frac{h+1}{3}\right)\right]\sum_{P=0}^{\frac{Q-2}{2}}\cos 2\pi P=2A\left\{\left[1-2\cos\pi\frac{2h+1}{3}\right]\right\}\frac{Q}{2}$$

so that:

$h = 1(\text{mod } 3)$: $F = N'A$

$h = 2(\text{mod } 3)$: $F = 0$

$h = 0(\text{mod } 3)$: $F = 0$

c. $l = 2Q(\text{mod } 3Q)$.

$$F=2A\sum_{P=0}^{\frac{Q-2}{2}}\left[\cos 4\pi P+\cos 2\pi\left(\frac{h}{3}-\frac{6P+2}{3}\right)+\cos 2\pi\left(\frac{h}{3}+\frac{6P+4}{3}\right)\right]=$$

$$=2A\left[1+\cos 2\pi\left(\frac{h-2}{3}\right)+\cos 2\pi\left(\frac{h+4}{3}\right)\right]\sum_{P=0}^{\frac{Q-2}{2}}\cos 2\pi P=2A\left\{\left[1+2\cos\pi\frac{2h+2}{3}\right]\frac{Q}{2}\right\}$$

so that:

$h = 1(\text{mod } 3)$: $F = 0$

$h = 2(\text{mod } 3)$: $F = N'A$

$h = 0(\text{mod } 3)$: $F = 0$

d. $l = 0(\text{mod } 3Q)$.

$$F=2A\sum_{P=0}^{\frac{Q-2}{2}}\left[\cos 6\pi P+\cos 2\pi\left(\frac{h}{3}-3P+1\right)+\cos 2\pi\left(\frac{h}{3}+3P+2\right)\right]=$$

$$=2A\left[1+\cos 2\pi\left(\frac{h}{3}-1\right)+\cos 2\pi\left(\frac{h}{3}+2\right)\right]\sum_{P=0}^{\frac{Q-2}{2}}\cos 2\pi P=2A\left\{\left[1+2\cos\pi\frac{2h}{3}\right]\frac{Q}{2}\right\}$$

so that:

$h = 1(\text{mod } 3)$: $F = 0$

$h = 2(\text{mod } 3)$: $F = 0$

$h = 0(\text{mod } 3)$: $F = N'\text{A}$

The complete result is:

$l_{C_1} \neq 0(\text{mod } N')$: $F = 0$

$l_{C_1} = (N'/3)h(\text{mod } N')$: $F = N'A$ (A2)

2. *Q = 2M-1*. With respect to the $Q = 2M$ case, the following differences exist:

a) the $(-1)^l$ does not appear;

b) there is one $u_x(m) = 1$ term less than those with $u_x(m) = 0$ and $u_x(m) = -1$

Eq. (A1) is thus simplified as follows:

$$F=A\left\{-1+2\sum_{P=0}^{\frac{Q-1}{2}}\cos 2\pi\frac{Pl}{Q}+\sum_{P=0}^{\frac{Q-1}{2}}\cos 2\pi\left(\frac{h}{3}-\frac{3P+1}{3Q}l\right)+\sum_{P=0}^{\frac{Q-3}{2}}\cos 2\pi\left(\frac{h}{3}+\frac{3P+2}{3Q}l\right)\right\} \quad \text{(A3)}$$

Proceeding as shown in the previous case, Eq. (A2) is obtained again.

A. 1. 2 All-even layers.

The only difference with respect to the all-odd case is the +/- sign exchange in the two terms containing $h/3$ in Eq. (A1) and (A3). The result is thus:

$l_{C_1} \neq 0(\text{mod } N')$: $F = 0$

$$l_{C_1} = (2N'/3)h(\text{mod } N'): F = N'A \qquad \text{(A4)}$$

A. 1. 3 Results.

From Eq. (A2) and (A4) it follows that:

1) an N-layer polytype belonging to subfamily A shows one reflection out of N in all the reciprocal lattice rows parallel to c^* corresponding to *family reflections;*
2) in the space-fixed reference, for all-odd layers polytypes the reflection condition is $l_{C_1} = (N'/3)h(\text{mod } N')$, while for all-even layers polytypes it is $l_{C_1} = 2(N'/3)h(\text{mod } N')$;
3) the diffraction pattern has to be rotated by 180° around the normal to the layer in order to match the *family reflections* for polytypes built by layers with opposite parity. This corresponds to the fact that the rhombohedral cell of the superposition structure is in the obverse setting for odd parity of the layers, but in the reverse setting for even parity of the layers, as can be seen from Fig. 3 in Ďurovič *et al.* (1984).

A. 2 Subfamily B.

The u_x component, being a sum of an even number of alternating -1 and 1, is always zero [see Table 3 and Eq. (7)]: subfamily B polytypes can thus be orthogonal ($N' = N$) or *Class b* polytypes ($N' = 3N$), but they cannot belong to *Class a*. In Eq. (2B) the first term is 1, the ($N'/2$)-th one is $(-1)^l$; the remaining ones form pairs $u_z(m)$ and $u_z(N'-m) = -u_z(m)$. Dividing polytypes for which $N' = 4M$ and those for which $N' = 4M+2$, Eq. (2B) can be re-written as follows.

$N' = 4M$

$$F = A\left\{1+(-1)^l+\sum_{m=1}^{M-1}\left[\exp 2\pi i\left(\frac{ml}{2M}\right)+\exp 2\pi i\left(-\frac{ml}{2M}\right)\right]\right\}+$$

$$A'\left\{\sum_{m'=1}^{M}\left[\exp 2\pi i\left(\frac{2m'-1}{2M}\,l\right)+\exp 2\pi i\left(-\frac{2m'-1}{2M}\,l\right)\right]\right\} =$$

$$A\left[1+(-1)^l+2\sum_{m=1}^{M-1}\left(\cos\frac{m}{M}\pi l\right)\right]+A'\left[2\sum_{m'=1}^{M}\left(\cos\frac{2m'-1}{2M}\pi l\right)\right]=AK_{4M}+A'K'_{4M}$$

$N' = 4M+2$

$$F = A\left\{1+\sum_{m=1}^{M}\left[\exp 2\pi i\left(\frac{ml}{2M+1}\right)+\exp 2\pi i\left(-\frac{ml}{2M+1}\right)\right]\right\} +$$

$$A'\left\{(-1)^l+\sum_{m'=1}^{M}\left[\exp 2\pi i\left(\frac{2m'-1}{4M+2}\,l\right)+\exp 2\pi i\left(-\frac{2m'-1}{4M+2}\,l\right)\right]\right\} =$$

$$A\left[1+2\sum_{m=1}^{M}\left(\cos\frac{2m}{2M+1}\pi l\right)\right]+A'\left[(-1)^l+2\sum_{m'=1}^{M}\left(\cos\frac{2m'-1}{2M+1}\pi l\right)\right]=AK_{4M+2}+A'K'_{4M+2}$$

When $l = 0(\text{mod } N')$ all the terms under summation go to 1, so that $K_{4M} = K'_{4M} = 2M = N'/2$, $K_{4M+2} = K'_{4M+2} = 2M+1 = N'/2$. When $l = (N'/2)(\text{mod } N')$ all the terms under summation in the expression of K_{4M} and K_{4M+2} again go to 1, so that $K_{4M} = 2M = N'/2$, $K_{4M+2} = 2M+1 =$

$N'/2$. However, in the expression of K'_{4M} and K'_{4M+2} all the terms under summation go to -1 and thus K_{4M} -2M = -$N'/2$, K_{4M}+2 = -(2M+1) = -$N'/2$.

When $l \neq 0(\text{mod } N'/2)$ the following simplified expressions are easily obtained :

$$K_{4M}=-1+(-1)^l+2\left[1+\sum_{m=1}^{M-1}\cos\frac{m}{M}\pi l\right]=-1+(-1)^l+2\frac{\sin\frac{\pi l}{2}}{\sin\frac{\pi l}{2M}}\cos\left(\frac{M-1}{M}\frac{\pi l}{2}\right)=$$

$$=-1+(-1)^l+2\frac{\sin\frac{\pi l}{2}}{\sin\frac{\pi l}{2M}}\left(\cos\frac{\pi l}{2}\cos\frac{\pi l}{2M}+\sin\frac{\pi l}{2}\sin\frac{\pi l}{2M}\right)=-1+(-1)^l+2\left(\frac{\sin\frac{\pi l}{2}}{\sin\frac{\pi l}{2M}}\cos\frac{\pi l}{2}\cos\frac{\pi l}{2M}+\sin^2\frac{\pi l}{2}\right)=0$$

$$K'_{4M}=2\sum_{m'=1}^{M}\cos\frac{2m'-1}{2M}\pi l=2\frac{\sin\pi l}{\sin\frac{\pi l}{2M}}=0$$

$$K_{4M+2}=-1+2\left[1+\sum_{m=1}^{M}\cos\frac{2m}{2M+1}\pi l\right]=-1+2\frac{\sin(M+1)\frac{\pi l}{2M+1}}{\sin\frac{\pi l}{2M+1}}\cos\left(M\frac{\pi l}{2M+1}\right)=0$$

$$K'_{4M+2}=(-1)^l+2\sum_{m'=1}^{M}\cos\frac{2m'-1}{2M+1}\pi l=(-1)^l+\frac{\sin\frac{2M\pi l}{2M+1}}{\sin\frac{\pi l}{2M}}=(-1)^l+\frac{-\cos\frac{\pi l}{2}\sin\frac{\pi l}{2M}}{\sin\frac{\pi l}{2M}}=(-1)^l-(-1)^l=0$$

(the trigonometric term in the expression of K_{4M+2} is always 0.5).

Finally:

$$\begin{aligned} &l\neq 0\left(mod\ \frac{N'}{2}\right): && F=0\\ &l=\frac{N'}{2}\ (modN'): && F=N'\frac{A-A'}{2}\neq 0\\ &l=0(modN'): && F=N'\frac{A+A'}{2}\neq 0 \end{aligned} \qquad \text{(A5)}$$

and the reflection conditions are:

$$\begin{aligned} &h=0(\text{mod } 3): && l_{C_1}=0(\text{mod } N')\\ &h\neq 0(\text{mod } 3): && l_{C_1}=0(\text{mod } N'/2) \end{aligned} \qquad \text{(A6)}$$

Acknowledgments–This research has been partly developed during a Doctoral Program supported by the Japanese Ministry of Education, Science and Culture, and the results were partly obtained when the author was guest of the Russian Academy of Sciences in Moscow (June 1997). The author expresses his deep gratitude to Prof. Boris B. Zvyagin (IGEM, RAS, Moscow) and to Prof. Slavomil Ďurovič (Slovak Academy of Sciences, Bratislava) for many valuable discussions. Special thanks to Prof. Giovanni Ferraris (University of Torino) for critical reading of a previous version of the manuscript. Two anonymous referees gave several important suggestions and comments, which allowed the author to improve the clearness of the manuscript and to make more consistent the treatment. The

author is indebted to Prof. Hiroshi Takeda (Chiba Institute of Technology), Prof. Yoshio Takéuchi (Nihon University, Tokyo), Prof. Ryoichi Sadanaga (Japan Academy), Dr. T. Kogure (University of Tokyo), and Prof. Stefano Merlino (University of Pisa) for discussions; Prof. Dmitry Yu. Pushcharovsky (Moscow State University) for sending consultation material; Prof. Masamichi Miyamoto (University of Tokyo) and Prof. Yasunari Watanabe (Teikyo Heisei University) for constant encouragement.

References.

ARNOLD, H.(1996) *Transformations in crystallography*. Sect. 5 in *International Tables for Crystallography,* Vol. A (Ed. Theo Hahn). Dordrecht / Boston / London: Kluwer Academic Publishers, 69–80.

BACKHAUS, K. -O. and ĎUROVIČ, S. (1984) Polytypism of micas. I. MDO polytypes and their derivation. *Clays Clay Miner.*, **32**, 453–463.

BAILEY, S. W. (1975) Cation Ordering and Pseudosymmetry in Layer Silicates. *Am. Mineral.*, **60,** 175–187.

BAILEY, S. W. (1984) Review of Cation Ordering in Micas. *Clays Clay Miner.*, **32**, 81–92.

BELOV, N. V. (1949) The twin laws of micas and micaceous minerals. *Mineralog. sb. L'vovsk. geol. obva pri. univ.*, **3**, 29–40 (in Russian).

BORUTSKIY, B. Y., SOBOLEVA, S. V. and GOLOVANOVA, T.I. (1987) Three-layered 3Tc biotite from the Khibiny pluton. *Transactions (Doklady) U. S. S. R. Acad. Sciences: Earth Science Section*, **294,** 141–143.

BUERGER, M. J. (1954) The diffraction symmetry of twins. *Anaias de Acad. Bras. de Ciencias,* **26**, 111–121.

CATTI, M. and FERRARIS, G. (1976) Twinning by Merohedry and X-ray Crystal Structure Determination. *Acta Crystallogr.*, **A32**, 163–165.

DONNAY, G., MORIMOTO, N., TAKEDA, H. and DONNAY, J. D. H. (1964) Trioctahedral One-Layer Micas. I. Crystal Structure of a Synthetic Iron Mica *Acta Crystallogr.*, **17**, 1369–1373.

DORNBERGER-SCHIFF, K. (1959) On the nomenclature of the 80 plane groups in three dimensions. *Acta Crystallogr.*, **12**, 173.

DORNBERGER-SCHIFF, K. (1964) *Grundzuge einer Theorie von* OD-Strukturen aus Schichten. Abh. dtsch. Akad. Wiss. Berlin, Kl. f. Chem. 3.

DORNBERGER-SCHIFF, K. (1966) *Lehrgang uber OD-strukturen*. Berlin: Akademie-Verlag.

DORNBERGER-SCHIFF, K. (1979) OD Structures, - a Game and a Bit more. *Kristall und Technik,* **14**, 1027–1045.

DORNBERGER-SCHIFF, K., BACKHAUS, K. -O. and ĎUROVIČ, S. (1982) Polytypism of micas: OD-Interpretation, Stacking symbols, Symmetry Relations. *Clays Clay Miner.*, **30**, 364–374.

ĎUROVIČ, S. (1992). *Layer stacking in general polytypic structures.* Sect. 9.2.2 in *International Tables for Crystallography*, Vol. C (Ed. A.C.J. Wilson) Dordrecht / Boston / London: Kluwer Academic Publishers, 667–680.

ĎUROVIČ, S. (1994a). Classification of phyllosilicates according to the symmetry of their octahedral sheets. *Ceramics-Silikaty*, **38**, 81-84.

ĎUROVIČ, S. (1994b) Significance of superposition structures in the polytypism of phyllosilicates. *In* Chapuis, G. and Paciorek, W. (Ed.) *Aperiodic '94. Proceedings of the International Conference on Aperiodic Crystals.* Singapore / New Jersey / London / Hong Kong : World Scientific, 595–599.

ĎUROVIČ, S. (1997) Fundamentals of OD theory. In Merlino, S. (Ed.) *Modular aspects of minerals / EMU Notes in Mineralogy,* Vol. 1. Budapest: Eötvös University press, 1–28.

ĎUROVIČ, S. and WEISS, Z. (1986) OD structures and polytypes. *Bull. Minéral.*, **109**, 15-29.

ĎUROVIČ, S., WEISS, Z. and BACKHAUS, K. -O. (1984) Polytypism of micas. II. Classification and abundance of MDO polytypes. *Clays Clay Miner.*, **32**, 454–474.

FICHTNER, K. (1977) Zur Symmetriebeschreibung von OD-Kristallstrukturen durch Brandtsche und Ehresmannsche Gruppoide. *Beitr. z. algebra u. Geometrie*, **6**, 71–99.

FILUT. M. A., RULE, A. C. and BAILEY, S. W. (1985) Crystal structure refinement of anandite-2*Or*, a barium- and sulfur-bearing trioctahedral mica. *Am. Mineral.*, **70**, 1298–1308.

FRIEDEL, G. (1904) *Étude sur les groupements cristallins.* Extrait du *Bullettin de la Societe de l'Industrie minerale*, Quatriéme série, Tomes III e IV. Saint-Étienne, Societè de l'Imprimerie Theolièr J. Thomas et C., 485 pp.

FRIEDEL, G. (1926) *Leçons de Cristallographie,* Berger-Levrault, Nancy, Paris, Strasbourg, XIX+602 pp.

GIUSEPPETTI, G. and TADINI, C. (1972). The Crystal Structure of 2*O* Brittle Mica: Anandite. *Tschermaks Min. Petr. Mitt.*, **18**, 169–184.

GOLDSCHMIDT, V. (1918) Atlas der Krystallformen, band IV. Heidelberg: Carl Winters Universitätsbuchhandlung.

GRELL, H. (1984) How to choose OD layers. *Acta Crystallogr.*, **A40**, 95–99.

GUINIER, A., BOKIJ, G. B., BOLL-DORNBERGER, K., COWLEY, J. M., ĎUROVIČ, S., JAGODZINSKI, H., KHRISNA, P., DEWOLFF, P. M., ZVYAGIN, B. B., COX, D. E., GOODMAN, P., HAHN, TH., KUCHITSU, K. and ABRAHAMS, S. C. (1984). Nomenclature of Polytype Structures. Report of the International Union of crystallography *Ad-Hoc* Committee on the Nomenclature of Disordered, Modulated and Polytype Structures. *Acta Crystallogr.*, **A40**, 399–404.

HAHN, TH. and VOS, A. (1996) *Reflection conditions.* Sect. 2.13 in *International Tables for Crystallography,* Vol. A (Ed. Theo Hahn). Dordrecht / Boston / London: Kluwer Academic Publishers, 27–30.

KOGURE, T. (1997) On the structure of cleaved surfaces in biotite mica. *Mineral. J.*, **19**, 155–164.

KOGURE, T. and NESPOLO, M. (1999a) First occurrence of a stacking sequence including (±60°, 180°) rotations in Mg-rich annite. *Clays Clay Miner.*, **47** (in press).

KOGURE, T. and NESPOLO, M. (1999b) A TEM study of long-period mica polytypes: determination of the stacking sequence of oxybiotite by means of atomic-resolution images and Periodic Intensity Distribution (PID). *Acta Crystallogr.* **B55** (in press).

LE PAGE, Y. (1982) The Derivation of the Axes of the Conventional Unit Cell from the Dimensions of the Buerger-Reduced Cell. *J. Appl. Crystallogr.*, **15**, 255–259.

MCLARNAN, T. J. (1981) The number of polytypes in sheet silicates. *Z. Kristallogr.*, **155**, 247–268.

MERLINO, S. (1990) OD structures in mineralogy. *Per. Mineral.*, **59**, 69–92.

MOGAMI, K., NOMURA, K., MIYAMOTO, M., TAKEDA, H. and SADANAGA, R. (1978) On the Number of Distinct Polytypes of Mica and SiC with a Prime Layer-Number. *Can. Mineral.*, **16**, 427–435.

MÜLLER, K. and CHANG, C. C. (1969) Electric dipoles on clean mica surfaces. *Surface Science*, **14**, 39–51.

NESPOLO, M. (1998) Discovery of a complex mica polytype belonging to non-basic structural series, and its formation mechanism. Doctoral dissertation, University of Tokyo, 257 p.

NESPOLO, M. and KOGURE, T. (1998) On the indexing of 3*T* mica polytype. *Z. Kristallogr.*, **213**, 4–12.

NESPOLO, M. and TAKEDA, H. (1999) Inhomogeneous mica polytypes: 8-layer polytype of the $2M_1$ structural series determined by the Periodic Intensity Distribution (PID) analysis of the X-ray diffraction pattern. Submitted to *Mineral. J.*

NESPOLO, M., TAKEDA, H. and FERRARIS, G. (1997a) Crystallography of mica polytypes. *In* Merlino, S. (Ed.) *Modular aspects of minerals / EMU Notes in Mineralogy*, Vol. 1. Budapest: Eötvös Univer-

sity press, 81–118.

NESPOLO, M., TAKEDA, H., FERRARIS, G. and KOGURE, T. (1997b) Composite twins of 1*M* mica: derivation and identification. *Mineral. J.*, **19,** 173–186.

NESPOLO, M., TAKEDA, H. and FERRARIS, G. (1998) Representation of the axial settings of mica polytypes. *Acta Crystallogr.*, **A54**, 348–356.

NESPOLO, M., KOGURE, T. and FERRARIS, G. (1999a) Allotwinning: oriented crystal association of polytypes - some warnings of consequences. *Z. Kristallogr.*, **214**, 5–8.

NESPOLO, M., TAKEDA, H., KOGURE, T. and FERRARIS, G. (1999b) Periodic Intensity Distribution (PID) of mica polytypes: symbolism, structural model orientation and axial settings. *Acta Crystallogr.*, **A55** (in press).

NI, Y. and HUGHES, J. M. (1996) The crystal structure of nanpingite-$2M_2$, the Cs-end member of muscovite. *Am. Mineral.*, **81**, 105–110.

PABST, A. (1955) Redescription of the single layer structure of the micas. *Am. Mineral.*, **40**, 967–974.

PAULING, L. (1930) The structure of micas and related minerals. *Proc. Nat. Ac. Sci. Washington*, **16**, 123–129.

PAVESE, A., FERRARIS, G., PRENCIPE, M. and IBBERSON, R. (1997) Cation site ordering in phengite 3T from the Dora-Maira massif (western Alps): a variable-temperature neutron powder diffraction study. *Eur. J. Mineral.*, **9**, 1183–1190.

RADOSLOVICH, E. W. (1959) Structural control of Polymorphism in Micas. *Nature*, **163**, 253.

RADOSLOVICH, E. W. (1961) Surface symmetry and cell dimensions of layer-lattice silicates. *Nature,* **191**, 67–68.

RIEDER, M. (1968) Zinnwaldite: Octahedral Ordering in Lithium-Iron Micas. *Science*, **160**, 1338–1340.

ROSS, M., TAKEDA, H. and WONES, D. R. (1966) Mica Polytypes: Systematic Description and Identification. *Science*, **151**, 191–193.

SADANAGA, R. and TAKEDA, H. (1968) Monoclinic Diffraction Patterns Produced by Certain Triclinic Crystals and Diffraction Enhancement of Symmetry. *Acta Crystallogr.*, **B24**, 144–149.

SADANAGA, R. and TAKEDA, H. (1969) Description of Mica Polytypes by New Unit Layers. *J. Mineral. Soc. Japan*, **9,** 177-184 (in Japanese).

SADANAGA, R. and TAKÉUCHI, Y. (1961) Polysynthetic twinning of micas. *Z. Kristallogr.*, **116**, S. 406–429.

SMITH, J. V. and YODER, H. S. (1956) Experimental and Theoretical Studies of the mica polymorphs. *Mineral. Mag.*, **31**, 209–235.

SMRČOK, Ľ., ĎUROVIČ, S., PETŘÍČEK, V. and WEISS, Z. (1994) Refinement of the crystal structure of cronstedtite-3T. *Clays Clay Miner.*, **42**, 544–551.

TAKANO, Y. and TAKANO, K. (1958) Apparent polytypism and Apparent Cleavage of the Micas. *J. Mineral. Soc. Japan*, **3**, 674–692 (in Japanese).

TAKEDA, H. (1967) Determination of the Layer Stacking Sequence of a New Complex Mica Polytype: A 4-layer Lithium Fluorophlogophite. *Acta Crystallogr.*, **22**, 845–853.

TAKEDA, H. and BURNHAM, C. W. (1969) Fluor-polylithionite: a lithium mica with nearly hexagonal $(Si_2O_5)^{2-}$ ring. *Mineral. J.*, **6**, 102–109.

TAKEDA, H. and ROSS, M. (1995) Mica Polytypism: Identification and Origin. *Am. Min.*, **80**, 715–724.

TAKEDA, H. and SADANAGA, R. (1969) New Unit Layers for Micas. *Mineral. J.*, **5**, 434–449.

TAKÉUCHI, Y. (1971) Polymorphic or polytypic changes in biotites, pyroxenes, and wollastonites. *J. Mineral. Soc. Japan*, **10**, Spec. Issue No. 2, 87–99 (in Japanese).

TAKÉUCHI, Y. and HAGA, N. (1971) Structural Transformation of Trioctahedral Sheet Silicates. Slip mechanism of octahedral sheets and polytypic changes of micas. *Mineral. Soc. Japan Spec. Pap.*,

1 (1971) 74-87 (Proc. IMA-IAGOD Meetings '70, IMA Vol.).

WEISS, Z. and WIEWIÓRA, A. (1986) Polytypism of Micas. III. X-ray Diffraction Identification. *Clays Clay Miner.*, **34**, 53–68.

ZHUKHLISTOV, A. P., LITSAREV, M. A. and FIN'KO, V. I. (1993) First Find of a Six-Layered Triclinic 6*Tc* Polytype of a Ti-Oxybiotite. *Trans. (Doklady) Russ. Acad. Sci., Earth Science Sect.*, **329**, 188–194.

ZHUKHLISTOV, A. P., ZVYAGIN, B. B., SOBOLEVA, S. V. and FEDOTOV, A. F. (1973) The crystal structure of the dioctahedral mica $2M_2$ by high voltage electron diffraction. *Clays Clay Miner.*, **21**, 465–470.

ZHUKHLISTOV, A. P., ZVYAGIN, B. B. and PAVLISHIN, V. I. (1990). Polytypic 4M modification of Ti-biotite with nonuniform alternation of layers, and its appearance in electron-diffraction patterns from textures. *Sov. Phys. Crystallogr.*, **35**, 232–236.

ZVYAGIN, B. B. (1957) Determination of the structure of celadonite by electron diffraction. *Sov. Phys. Crystallogr.*, **2**, 388–394.

ZVYAGIN, B. B. (1967) *Electron diffraction analysis of clay mineral structures*. New York: Plenum Press, XVI+364 pp.

ZVYAGIN, B. B. (1974) The use of symbolic structure notations for deduction of equivalence, symmetry and diffraction properties of the layer silicates. 2^{nd} *Eur. cryst. Meet. Coll. Abstracts, Keszthely,* 162–164.

ZVYAGIN, B.B. (1985) Polytypism in contemporary crystallography. Sov. Phys. Crystallogr., 32, 394–399.

ZVYAGIN, B. B. (1993) A contribution to polytype systematics. *Phase transitions*, **43**, 21–25.

ZVYAGIN, B. B. (1997) Modular analysis of crystal structures. *In* Merlino, S. (Ed.) *Modular aspects of minerals / EMU Notes in Mineralogy*, Vol. 1. Budapest: Eotvos University press, 345–372.

ZVYAGIN, B. B., VRUBLEVSKAYA, Z. V., ZHUKHLISTOV, A. P., SIDORENKO, O. V. SOBOLEVA, S. V. and FEDOTOV, A. F. (1979) *High-voltage electron diffraction in the study of layered minerals.* Moscow: Nauka Press, 223 pp. (in Russian).

Received February 12, 1998; accepted April 26, 1999